



DEPARTMENT OF MARINE TECHNOLOGY

MASTER THESIS

Offshore Wind Turbine Modelling State of The Art and future development

Author:
Florian Saberniak

Supervisor:
Amir R. Nejad

June, 2022

Preface

This document presents a state of the art review of modelling methods and tools and methods, current state of the offshore wind market and outlook, industry standards, a system description of floating wind turbines, theoretical background and a description of how to model the system components considering a fully coupled model including drive-train dynamics. The research aims to provide a framework on how to model floating wind turbines using Multi-body Simulation and considers the fidelity needed to create a satisfactory model resulting in realistic results when running the simulations. SIMPACK is especially considered, and an extensive review of previous work is conducted to create the updated recommendations on model fidelity of the floating wind turbine components. System components include blades, drive-train, tower, foundation and mooring lines.

I would like to thank Amir R. Nejad for the guidance and continued support through these hard times. I would also like to thank the faculty for allowing me to submit the thesis. I pray that this will conclude my time as a student and that the world allows me to see its small miracles again.

The topics are represented in the following order:

- Section 1: Introduction
- Section 2: Theory and Modelling Framework
- Section 3: Standards
- Section 4: Development Trend
- Section 5: Discussion
- Section 6: Conclusion
- Section 7: Further work

1 Abstract

The master thesis presents the state-of-the-art technologies and development trends of wind turbines. Offshore wind is seen as a promising energy sector in the shift towards renewable energy sources. DNVs forecast for 2050 shows that offshore wind turbines will contribute to 33 percent of the global energy supply with floating offshore wind turbines being 4 percent of global energy supply. To lowering the levelized cost of energy for offshore wind the upscaling of turbine size of significance. As of today the operational costs of floating wind farms is 5 times higher than a bottom fixed offshore wind turbine farms. The requirements for the floating support structure often leads to twice the amount of steel needed. Increasing the size of the turbine and researching new design concepts require advanced tools for modeling and analysing the loads on the system components. A fully coupled multi-body-simulation approach is researched. The approach includes both wind and wave loads. Various software for modeling and simulation currently available are researched. The theory required and state-of-the-art on modeling the various system components are presented. Standards such as the IEC 61400 series and a number of DNV standards are studied to see if there are gaps between the rules and standards and the current wind turbine development. There were several gaps as standards were limited to smaller wind turbines. There is however constant development and new editions are being released by the regulatory bodies. These new editions include larger floating wind turbines, but might not include standards for vertical axis turbines, shared anchoring wind turbines and multiple turbines supported by a single floating structure. As turbine size grows the rotor speed decreases. This makes direct drive generators a valid option instead of using gearboxes. The gearbox is the drivetrain component with the highest failure rate and causes most downtime. This is one of the factors that might reduce the operational costs making floating offshore wind better suited for the future.

Contents

1 Abstract	i
List of Figures	iv
2 Introduction	1
2.1 Problem description	1
2.2 Offshore Wind Outlook	1
2.3 Current floating Offshore Wind Turbine Projects	3
2.4 Offshore Wind Turbine System Description	3
2.4.1 Offshore Wind Turbine Foundation Variations	4
2.4.2 Floating platform	5
2.4.3 Mooring-system and Anchoring	6
2.4.4 Blades	7
2.4.5 Drivetrain	7
2.4.6 Tower	8
2.5 Resonance Frequency	8
3 Theory and Modelling Framework	9
3.1 Simulation Codes	9
3.2 Coupled vs De-coupled Approach	9
3.3 Multi-Body System (MBS) Simulation	10
3.4 Aerodynamics	12
3.4.1 Basic Aerodynamics	12
3.4.2 Momentum Theory	12
3.4.3 Wake rotation	12
3.4.4 Blade Element Momentum (BEM) Method	13
3.4.5 Background	13
3.4.6 Correction Factors	14
3.4.7 Tower Influence	16
3.4.8 Wind Input	16
3.4.9 AeroDyn in Simpack	17
3.4.10 Wind Turbine Control	17
3.5 Rotor Blade Generation	18
3.6 Structural Mechanics	18
3.6.1 Flexible Bodies	18

3.6.2	Structural Stresses	20
3.6.3	Rotor Blade Generation	20
3.7	Drivetrain Mechanics	21
3.7.1	Gearbox	21
3.7.2	Bearings	22
3.7.3	Additional Considerations	23
3.8	Structural Mechanics	24
3.8.1	Flexible Bodies	24
3.8.2	Structural Stresses	26
3.9	Hydrodynamics	26
3.9.1	Stability	26
3.9.2	Airy wave theory	26
3.9.3	Potential-flow theory	27
3.9.4	Morison	27
3.9.5	Wave spectrum	28
3.9.6	Wave frequency loads	29
3.9.7	Damping	29
3.9.8	Modelling Codes With Respect to Hydrodynamics	29
3.9.9	Modeling of floater	31
3.9.10	SIMPACK	31
3.10	Mooring System Modelling	33
3.10.1	SSI Modelling for bottom-fixed foundations	35
3.10.2	Soil Properties	37
3.10.3	Soil-Structure Interaction	38
3.10.4	Seabed Modelling	38
3.10.5	SSI Modelling	39
3.10.6	0-Degrees of Freedom	39
3.10.7	Multi-Degree of Freedom	39
4	Standards	40
4.1	Standards for Floating Wind Power Plants	40
4.2	ABS	41
4.3	DNV	42
4.4	IEC 61400 series	42
5	Development Trend	43

6 Discussion	44
7 Conclusion	45
8 Further work	46
9 Appendix	47
9.1 Appendix A	47
Bibliography	55

List of Figures

1	Wind Energy Cumulative Installed capacity in Europe (Wind Europe 2020)	2
2	Evolution of wind turbine size and power output (Pisanò 2019)	2
3	Floating wind status per 2020 (DNV 2020)	3
4	Diagram of Study Aspects (derived from NREL 2010)	4
5	Schematic of wind turbine foundations: a. pile foundation (on land); b. gravity foundation; c. monopile; d. suction bucket foundation; e. tripod foundation; f. jacket foundation; g. floating foundation(TLP). (X. Wang and Li 2020)	4
6	Assessment of floating platform classes (Cruz and Atcheson 2016)	6
7	Blade cost, power production and blade mass as blade length increases. (Willis et al. 2018)	7
8	A typical gearbox wind turbine drivetrain. (Taherian Fard et al. 2018)	8
9	Overview of FOWT Simulation Codes (Cruz and Atcheson 2016)	9
10	Decoupled drivetrain analysis method	10
11	1D Momentum Theory Diagram	12
12	Annular Plane	13
13	Blade Kinematics	14
14	Blade Kinetics	14
15	Glauert Correction for $F=1$	15
16	Tower Shadow	16
17	Typical FOWT Operation	17
18	Rotorblade Generation in SIMPACK	18
19	Blade Mode 1	19
20	SIMPACK EOM Update Process (Simpack 2020e)	20
21	Rotorblade Generation in SIMPACK	21
22	5MW High Speed Gearbox MBS Model Graphical Representation	22
23	5MW High Speed Gearbox MBS Model Topology	22

24	Force-deflection relation in bearings	23
25	Bearing Stiffness Matrix	23
26	Blade Mode 1	25
27	SIMPACK EOM Update Process (Simpack 2020e)	25
28	Boundary conditions for the linearized potential flow problem (Borg and Bredmose 2015)	27
29	Example of numerical tools (DNV-GL 2019)	30
30	Example of numerical tools(continued). (DNV-GL 2019)	31
31	DOFs of a floating wind turbine. (Ramachandran et al. 2013)	32
32	Schematic diagram of the MBS mooring line model (‘Offshore Wind Turbine Hydrodynamics Modeling in SIMPACK’ 2013), (Azcone et al. 2013)	34
33	MBS mooring line topology (Azcone et al. 2013).	35
34	SSI modelling of monopile in soil (Zuo et al. 2018)	36
35	Simplified foundation model of offshore monopile wind turbine in xz and xy planes (Sun and Jahangiri 2018)	36
36	Continuous vs. Discrete modeling of soil. (Gonzalez 2016)	37
37	Representative North Sea offshore soil profile. (Carswell et al. 2015)	37
38	Cable-seabed contact model (Azcone et al. 2013).	38
39	Simplified pile-soil interaction. (Xie et al. 2020)	39
40	Overview of floating wind standards (DNV-GL 2020)	40
41	Workflow for floating offshore wind (DNV 2022b)	44
42	Wind turbine relevant standards and other guidance documents, bottom-fixed (DNV-GL 2020)	47
43	Wind turbine relevant standards and other guidance documents, bottom-fixed (continued) (DNV-GL 2020)	48
44	Wind turbine relevant standards and other guidance documents, bottom-fixed (continued) (DNV-GL 2020)	49
45	Offshore substation relevant standards and other guidance documents (DNV-GL 2020)	49
46	Offshore substation relevant standards and other guidance documents (continued) (DNV-GL 2020)	50
47	Offshore substation relevant standards and other guidance documents (continued) (DNV-GL 2020)	51
48	Offshore substation relevant standards and other guidance documents (continued) (DNV-GL 2020)	52
49	Offshore substation relevant standards and other guidance documents (continued) (DNV-GL 2020)	53
50	Power cables relevant standards and other guidance documents (DNV-GL 2020)	53
51	Power cables relevant standards and other guidance documents (continued) (DNV-GL 2020)	54

2 Introduction

2.1 Problem description

As the world is moving towards renewable energy solutions floating offshore wind will play a big role. To have the ability to tackle the challenges the present and future brings it is crucial to have a broad understanding of the current market and limitations. This report presents the offshore turbine systems, how to model the system components and some underlying theory, current tools and approaches used in modeling and analysing floating offshore wind turbines, such as multi-body-simulation, and an overview of the current regulatory landscape. The results are discussed and some recommendations are presented.

The transition towards renewable and clean energy sources continues to be a global goal the offshore wind turbine industry is growing at a rapid pace. Currently there are standards and programs that can tackle the current situation, but in order to lower the cost of construction and operation the industry needs to develop. Both in terms of more wind turbines in a wind turbine park, but also in terms of the size of the wind turbines. Most of the turbines being operated today have a capacity around 5MW, but there are many plans of larger turbines with capacity of 15MW or more. This might require different technical solutions to those used today, such as direct drive power generation. The scaling in size set new requirements to all parts of the offshore wind turbine systems. It is therefore important to have the right tools and methods to design, model and analyze a floating offshore wind turbine. This will make it possible to do several design iterations at a higher pace and helps to avoid costly mistakes. The increase in size of all systems might also introduce new correlations in modal modes and natural frequencies. To tackle this problem a multi-body-simulation or MBS can be applied. There are also other approaches applicable and some of these are presented and discussed. As the global demand for energy increases so does the competition in creating the supply. A clear regulatory framework is therefore beneficial. Currently there are standards the has to be followed such as IEC61400 and a number of standards from DNV, such as DNVGL-ST-0119, DNVGL-ST-0376 and DNVGL-ST-0126. The standards and a further description is presented in the Standards-section.

2.2 Offshore Wind Outlook

The wind energy industry has been steadily growing for the last 15 years. The majority of installed power is still on land but there has been a growing interest for offshore wind turbine solutions in recent years. This can be seen in a European market analysis shown in Figure 1. There is also a trend for turbines to get larger with turbine power rating reaching more than 10MW, this is illustrated in Figure 2. The increase in size is mostly by reduction in maintenance and installation costs (Marsh 2005).

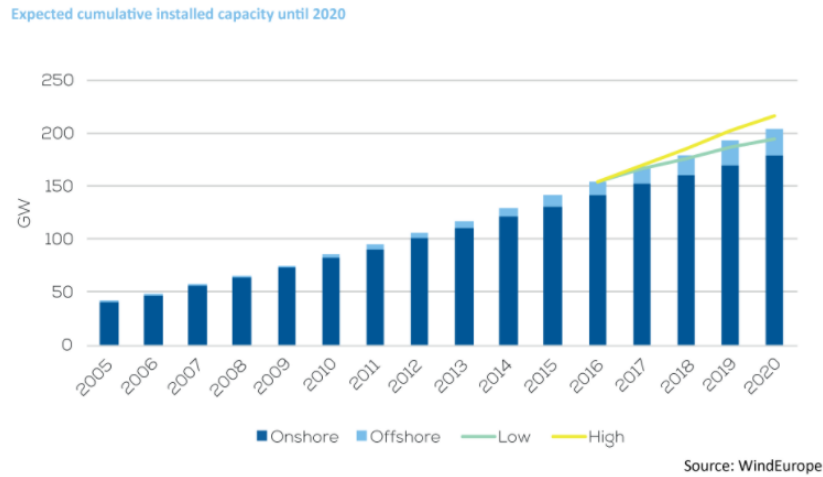


Figure 1: Wind Energy Cumulative Installed capacity in Europe (Wind Europe 2020)

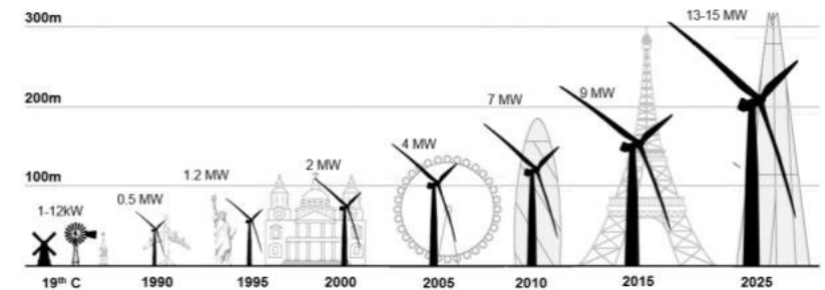


Figure 2: Evolution of wind turbine size and power output (Pisanò 2019)

The main factors contributing to the interest in offshore and floating installations can be identified as (derived from Kumar et al. 2016):

- Larger wind turbine sizes can be installed due to easier transport of parts when compared to on-shore
- The offshore wind conditions have higher velocities and are more stable due to less terrain shearing effects and turbulence
- There is less resistance from the public regarding disruption of landscapes and noise generation
- Larger areas available at lower prices

These advantages do not go without some additional challenges, such as:

- More complex system as the floating structure will add more degrees of freedom that can lead to additional damage to the structure.
- Corrosive environment that will affect the structural integrity of metallic components (tower, platform and mooring system)
- Difficult access for installation and maintenance dependent on favorable weather conditions (waves and wind).
- Longer cables required to bring the electricity production back to land

The cost of renewable energy sources continues to decline. The global installed offshore wind capacity was 29 GW in 2019 and will continue to rise to 1,748 GW by 2050. 15 percent of all offshore wind energy will by then be generated by floating offshore wind turbines (DNV 2022a).

2.3 Current floating Offshore Wind Turbine Projects

The largest current floating offshore wind farm is Hywind Tampen with an installed capacity of 88 MW. There are several other floating offshore wind farms such as WindFloat Atlantic in Portugal and Kingcardine and Hywind in Scotland. These wind farms are operating showing that the technology is technically feasible. Other floating wind farms have been pilots proving the design solutions.

Hywind Scotland has been operational since 2017 and was the worlds first commercial offshore wind farm and consists of five 6 MW spar type floating turbines with a total capacity of 30 MW.

The following figure illustrates the floating wind status per 2020. The illustration only includes countries in Europe, but there are also a great number of floating offshore wind farms globally.

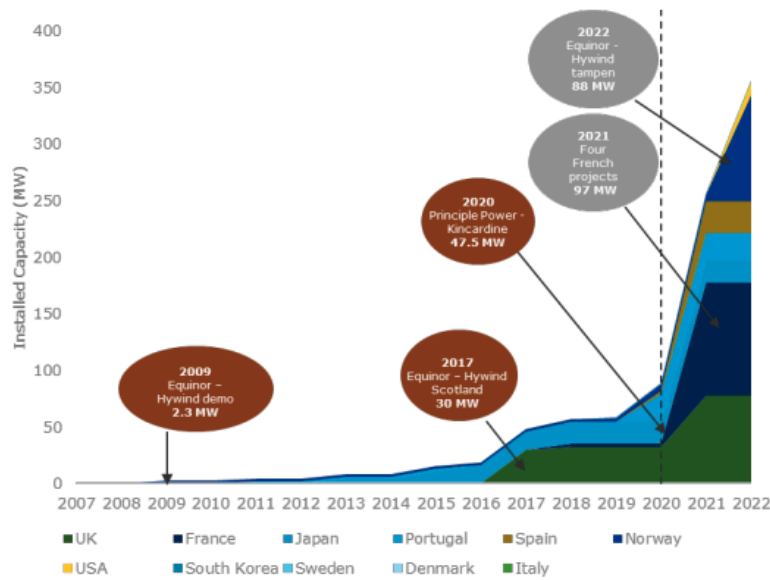


Figure 3: Floating wind status per 2020 (DNV 2020)

2.4 Offshore Wind Turbine System Description

The following sections will investigate several aspects for FOWT modelling. First, the various codes available will be presented for reference (Section 2). Then examples and theory required to build the model from the bottom up will be presented, this is graphically shown in Figure 4.

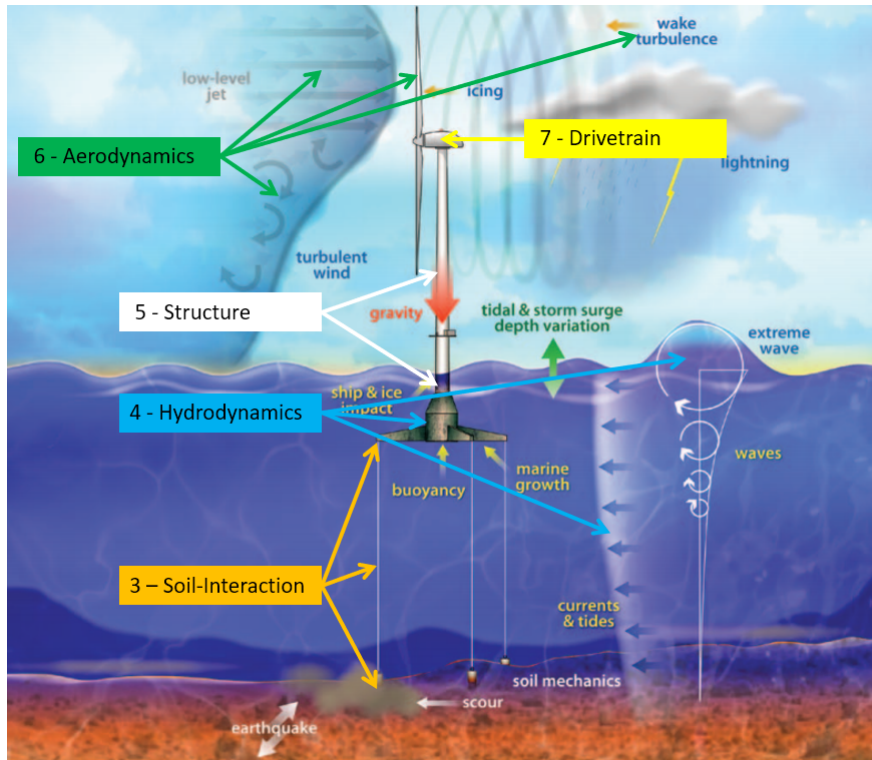


Figure 4: Diagram of Study Aspects (derived from NREL 2010)

2.4.1 Offshore Wind Turbine Foundation Variations

Most of the existing OWTs are supported by fixed foundation with water depth of less than 30 m (X. Wang and Li 2020). The most widely used support structure for OWT is the monopile foundation. There are however a number of different designs and variations for bottom fixed offshore wind turbine foundations. Selecting the foundation type is according to the turbine capacity, site environmental condition and geotechnical investigation. Fixed support structures are currently used in water depths < 60 m, but can be placed up to water depths of 80 m. As the water depth increases further the costs of design, construction and installation of the bottom fixed support structure is the main limitation. Variations of offshore foundations are represented in figure 5. The foundation design is chosen by two main factors; water depth and soil condition.

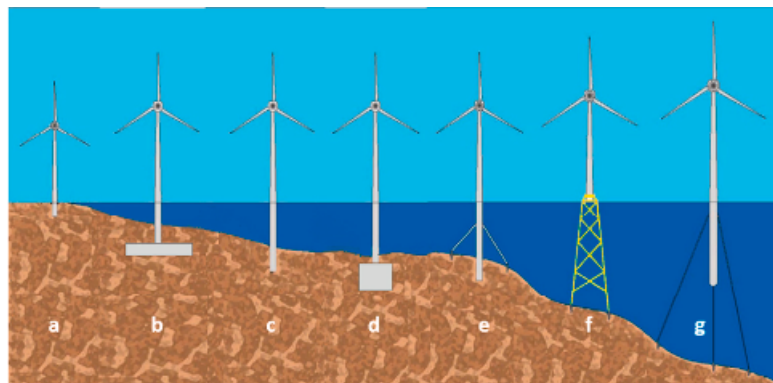


Figure 5: Schematic of wind turbine foundations: a. pile foundation (on land); b. gravity foundation; c. monopile; d. suction bucket foundation; e. tripod foundation; f. jacket foundation; g. floating foundation(TLP). (X. Wang and Li 2020)

Several other variations of both grounded and floating foundations is seen in (Igwemezie et al.

2019). Variations of mooring layout is also presented.

2.4.2 Floating platform

When looking at floating wind turbines, the soil-structure interaction cannot be modelled in the same fashion. The soil mainly interacts with the anchoring of the mooring system and the floating structure has a hydrodynamic interaction with the water. As the power production is moved further ashore where the water depth are > 80 m floating foundations are more suited. The floating structures raise a series of additional challenges for designers, as structures need to be evaluated for its stability, floatability and dynamic behavior. The most common types of these platforms include spar buoys, semi-submersibles and tension-leg-platforms.

The floating support structure consists of the following subsystems




- Structure (floater, platform): maintain buoyancy and structural integrity
- Mooring: connect the floater to the seabed, typically cables or chain
- Anchoring: attach the mooring lines to the seabed
- Electrical cable: transfer the electric power

The main structure must support the wind turbine and transmit loads while maintaining stability and station-keeping. The floating structure will experience several types of loads listed below.

- Wind-induced loads on the wind turbine rotor;
- Wave-induced loads on the floating structure;
- Ocean current induced loads;
- Weight of floater and wind turbine;
- Accident and fault loads;
- Other incidental loads such as dynamic response of export cable.

There are three major sources of stability for floating platforms (Stewart and Lackner 2013). The sources used too counter the loads are often a combination of the three, but the dominant one determines the basic shape of the foundation (Cruz and Atcheson 2016).

- Ballast stabilised: results in slender vertical structure (spar platform), has slow and small motions from waves, relatively easy to install but require large water depths;
- Buoyancy-stabilised, through hydrostatics: leads to a large surface structure (semi-submersible platform), suited for more shallow waters and relatively easy installation;
- Mooring-stabilised, through taut lines: leads to a slender highly loaded submerged structure (tension-moored or tension-leg platform), difficult installation, flexible water depths, small motions, less material (steel/concrete) requirements.

	Spar	TLP	Semi-Sub
			
Stability	Ballast	Moorings	Hydrostatics
Min depth ^a	Deeper	Shallower	Shallower
Periods	Good	Good	Acceptable
Cost	Uncertain	Uncertain	Uncertain
Yaw and torque	Acceptable	Probably good	Good
Fabrication	Potentially simple structure	More complex structure	More complex structure
Installation	More complex operation	More complex operation	Good

^aHowever greater depths will typically allow a better performing and lower cost design to be deployed

Figure 6: Assessment of floating platform classes (Cruz and Atcheson 2016)

Designing wind turbines with high performance requires high-fidelity analysis of the wind turbine characteristics. The analysis tool should be multi-functional and flexible to ensure that the user can explore various design details and frameworks. General multi-body modeling tools provides multidisciplinary method to complicate system modeling, which has made it an inevitable choice to solve these problems (Xie et al. 2020).

Regardless of the design chosen, the platform systems are designed to prevent excessive pitching of the turbine due to wind thrust, comply with loads applied (ULS, ALS, FLS), be cost effective and have a natural period that does not resonate with other parameters such as the rotor rotation (1P and 3P) and the environmental conditions (waves and wind).

2.4.3 Mooring-system and Anchoring

The mooring lines of a FOWT connects the floating foundation with the seabed in order to keep the structure in its desired location. There are several ways to design the mooring system, and chosen design affects how the dynamics of the FOWT is influenced. A brief, general overview of the mooring system components, based on (Cruz and Atcheson 2016), is presented below. More detailed descriptions of mooring system components are found in Cruz and Atcheson 2016.

- Mooring line: Chain, wire rope or fibre rope
- Anchor: drag embedment anchor, plate anchor, suction pile, pile and screw anchor, gravity anchor.
- Clump weight and buoyancy modules.
- Connection equipment and hardware: triplate, shackle, splices.

The number of mooring lines, chosen anchors and layout may greatly depending on floater design. Some variations are seen in Igwemezie et al. 2019. Catenary moored spar type is the most commonly used configuration. It consists of a single floating cylindrical spar-buoy moored by catenary cables (Barooni et al. 2018).

2.4.4 Blades

The blades are designed to generate aerodynamic lift, which is transformed into electricity by a generator. The blades are fabricated from composite materials (Willis et al. 2018). The materials and production of the turbine blades represent a substantial cost component of the levelized cost of energy for the wind energy. The design is driven by two conflicting demands. One is the demand of structural capability and the other is aerodynamic efficiency. An increase in blade length increases the swept rotor area which increases the energy capture. Longer blades means higher structural loads, which results in more slender blade designs in order to reduce material usage and blade loads (Willis et al. 2018). New materials and material characterization can offer a meaningful cost reduction as 50 percent of the cost of a manufactured blade is comprised of materials. The rotor diameter of global offshore wind turbines is typically 153 meters. Blade manufacturing is labor-intensive and 30 percent of the cost is labor costs. The following figure shows blade mass, blade cost and power production as blade length increases.

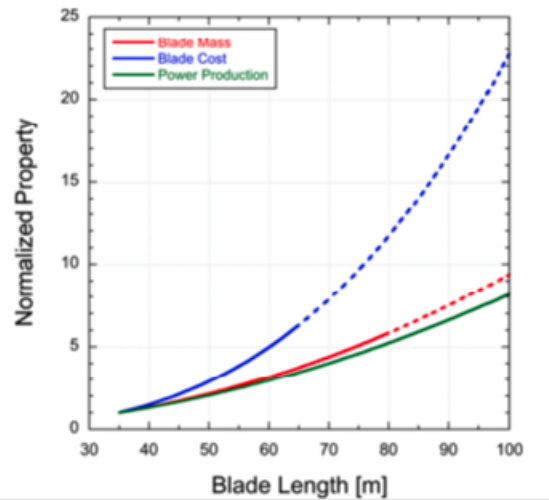


Figure 7: Blade cost, power production and blade mass as blade length increases. (Willis et al. 2018)

2.4.5 Drivetrain

The drivetrain is comprised of gearboxes, rotors and generators and is the highest cause of reliability and operational problems for a operating wind turbine. The rotating blades capture the wind power which is transmitted to the gearbox by the main shaft. The gearbox amplifies the speed so that the generator can convert the mechanical power into electrical energy. The high loads on the gears in the gearbox is a frequent cause of mechanical failures. Typically gearboxes cause the longest downtime per failure, which increases the levelized cost of energy. This is because of the loads and high number of components such as gears and bearings. To increase the overall system reliability a reduced number of parts would be beneficial. An option to achieve this is by implementing direct drive. The following figure shows a typical model of a drivetrain.

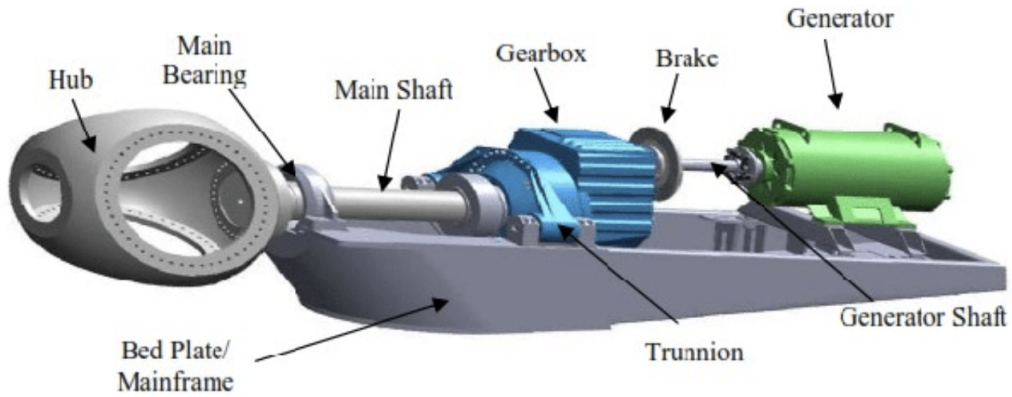


Figure 8: A typical gearbox wind turbine drivetrain. (Taherian Fard et al. 2018)

2.4.6 Tower

The tower support the turbine and present challenges to structural engineers. This is because of the combination of wind and wave loads derived in typical harsh offshore locations. The tower is connected to the floating foundation and the nacelle which results in loads due to movement of the floating support structure, wind, weight of the nacelle and blades and the rotation of the blades. As the blade length increases the height of the tower increases which introduces new requirements to the structural design. It is therefore important with improved models for analysing and optimizing the structural loads the structure has to withstand.

2.5 Resonance Frequency

A problem for FOWT may be that the rotor harmonic clashed with the structural frequencies. The blade passing frequency(3P) may clash with the frequency of other part which will cause significant fatigue damage on the tower. As the turbines become larger and rotate slower, a problem can arise when considering the motion of the floating platform as the resonance 1P may be close to the motion frequency.

3 Theory and Modelling Framework

The challenge when modelling a Floating Offshore Wind Turbine (FOWT) is the dynamic multi-physics environment in which it operates. It requires aero-hydro-servo-elastic simulations with non-linear forces varying in time. Each code uses a combination of methods, most of which have been extensively used in more mature industries such as hydrodynamics/mooring systems for offshore oil and gas, and aerodynamic methods from the aeronautical industry (Matha et al. 2011).

3.1 Simulation Codes

Many of the most popular simulation codes were developed for the design of onshore wind turbine devices with additional modules for the floating platforms and mooring systems. A summary of the main codes used today are summarized in Figure 10.

Code	Developer	Structural dynamics	Aerodynamics	Hydrodynamics	Mooring model
FAST v8	NREL	T: Mod/MB P: Rigid	(BEM or GDW) + DS	PF + ME	QS
SIMPACK + HydroDyn	SIMPACK	T: Mod/MB P: Rigid	BEM or GDW	PF + QD	QS
Bladed (Advanced Hydro Beta)	DNV GL	T: Mod/MB P: Rigid	(BEM or GDW) + DS	PF + ME + (IWL)	QS
Simo, Riflex + AeroDyn	MARINTEK, NREL	T: FE P: FE	(BEM or GDW) + DS	PF + ME	FE/Dyn
HAWC2	DTU Wind	T: MB/FE P: MB/FE	(BEM or GDW) + DS	ME	FE/Dyn

T turbine, *P* platform. *Mod* modal, *MB* multi-body, *FE* finite element, *BEM* blade element/momentum, *GDW* generalised dynamic wake, *DS* dynamic stall, *PF* potential flow *ME* Morison’s equation, *QD* quadratic drag, *IWL* instantaneous water level, *QS* quasi-static, *Dyn* dynamic

Figure 9: Overview of FOWT Simulation Codes (Cruz and Atcheson 2016)

Each method also has advantages and drawbacks mostly linked to the trade-off between simulation times versus the accuracy of the results. This is particularly true when comparing the computationally demanding Finite Element Methods (FEM) with rigid bodies. The development of these codes is also an academic combined effort to advance the FOWT industry. For example, modules from the NREL (National Renewable Energy Laboratory) FAST (Fatigue, Aerodynamic, Structures and Turbulence) code such as AeroDyn (Section 3.4) and HydroDyn (Section 3.9) are extensively used in other codes enabled by the modularization framework (J. Jonkman 2013).

The International Energy Agency (IEA) has conducted a global fixed and floating offshore wind turbine code comparison collaboration, titled "Task 30" based on a 5MW reference wind turbine by NREL (J. Jonkman et al. 2009). The OC3 (2005-2009) and OC4 (2010-2014) projects focused on verifying and bench-marking some of the aforementioned codes using code-code comparisons. This contributed to an overall increase in model accuracy (Popko et al. 2018). The OC5 project then continued the code validation by comparing with physical tank models. The current efforts (OC6) are being put on further validation based on obtaining real operational data from installed offshore wind turbines in collaboration with the industry (IEA Wind 2020).

3.2 Coupled vs De-coupled Approach

All the codes presented in the previous section provide coupling between selected loads. For example, the pitching motion of the platform affected by hydrodynamics forces will affect the aerodynamic inflow conditions to the rotor blades. Or for instance, the presence of the mooring lines will affect the stiffness and damping of the platform motions.

There are however very few FOWT models that include the coupling between the external (tower shadow, wind, waves) and the internal (gear mesh frequency) excitations. These excitations are typically respectively under 2Hz and above 20Hz. This de-coupling is valid as long as the drivetrain natural frequencies are higher than the external excitations (Peeters et al. 2006) and makes it

applicable when considering turbines with high speed gearboxes. A typical de-coupled approach as described in (Amir Rasekhi Nejad 2018) is shown in the following Figure. In this approach, the drivetrain is simplified to a two-three mass spring-damper model based on inertia and torsional stiffness. The global loading is then used as input to a more detailed gearbox model.

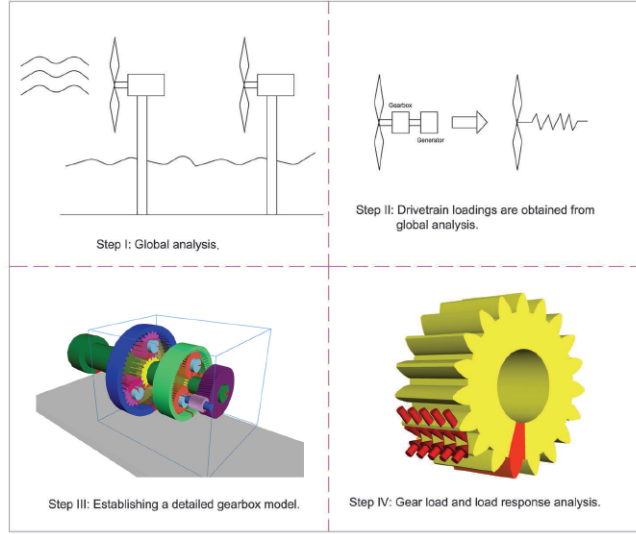


Figure 10: Decoupled drivetrain analysis method

On the other hand, there has been a growing interest in direct drives and medium speed gearbox drives for offshore applications, as the traditional high speed gearboxes have a higher failure rate, require more maintenance and cause a long downtime in case of failure (DTU Wind Energy Report 2013). When considering slower rotating drivetrains, there is a risk that the low external excitation frequencies and the internal excitation frequencies interfere with each other causing resonance. This is one of the motivations for this study.

The drawback of a fully coupled model is that it requires a small time step of around 0.005 seconds to capture the drivetrain dynamics even though 0.1 second would be sufficient to handle the environmental loads (Amir Rasekhi Nejad 2018). This will lead to much longer simulation times overall. The modelling approach and additional considerations are provided in Section 3.7.

Other coupling effects include the generator and control system dynamics. Some widely used simulation tools for these applications include; PSCAD/EMTDC to study the behaviour of electrical networks including the generator, frequency converter and transformers in transient operations. SIMULINK/MATLAB are also widely used for electrical system analysis as well as for control logic. Co-simulation between SIMULINK, PSCAD and the MBS programs presented below allows to further investigate the coupling effects between various systems within wind turbines (Uski et al. 2004).

3.3 Multi-Body System (MBS) Simulation

A multi-body system is a set of rigid or flexible bodies arranged in space with respect to global and local coordinate systems (markers). Each body is constrained with a specified number of degrees of freedom (joints) and interact with the environment or other bodies through the use of force elements (FE). This fundamental modelling approach is further detailed in (Shabana 2013). The MBS package that will be used in this study is the general purpose multibody simulation code SIMPACK developed by (Dassault Systemes 2020). It has wind turbine specific modules such as rotor blade generation, wind turbine control and interfaces to aerodynamic (AeroDyn) and hydrodynamic (HydroDyn) codes, this is further discussed in the subsequent sections. These modules will interact with the model with specific force elements, some dynamics can also be simplified with the use of spring/damper systems and directly applied forces.

The other main MBS simulation package on the market is ADAMS by (MSC Software 2020), both programs are based on the same core principles but there are some differences in the modeling approach. For example, in ADAMS all bodies are imported with 6 Degrees Of Freedom (DOF) and the constraints are determined by mathematical relationships to other DOF.

In SIMPACK, the user chooses the number of DOF required to describe the system (Blundell and Harty 2015). This ensures that no unnecessary constraints are being solved leading to a more efficient set of equations but requires correct engineering judgement in their selection.

The general calculation method within SIMPACK can be described as following, derived from (Rulka 1990) and similar to the equations of motion presented in the current SIMPACK documentation. For a given state, the formalism is given as:

- The second derivative of the positional coordinated: $\ddot{z} = g_1(\dot{z}, z, t)$
- The constraining forces and torques of the joint: $f^z = g_2(\dot{z}, z, t)$
- The applied forces and torques: $\dot{x} = g_3(x, \dot{z}, z, t)$
- Intermediate values of the laws of force for the applied forces
- Kinematic relative measurements (sensors for position, speed and acceleration)

The nonlinear equations are then linearized around a given state and/or a given initial position and initial speed. The eigenvalues and eigenvectors of the linear system matrix are calculated.

Lastly, a time-step integration is carried out to find solutions to the equations. The user can choose between several solvers. The default integrator is the SODASRT-2, it is recommended for the vast majority of cases due to being fast, accurate, robust and able to start from extreme non-equilibrium situations. It is a Backward Differentiation Formula (BDF) integrator that is suited for first and second order systems with positive damping. Instability can occur if the model is negatively damped or with higher order with low damping (Simpack 2020d)

The system can be time integrated in real time to get a visual representation of the system dynamics and can be ran offline in order to record the kinematics and kinetics that can be analyzed with the use of graphics.

Previous studies regarding the simulation of fixed and floating wind turbines using MBS methods include:

- (Beyer et al. 2013), in this article it was shown that SIMPACK coupled with HydroDyn showed that the platform motions caused by a decay test were similar to more advanced CFD results.
- (Withee 2004) used the MBS package ADAMS combined with AeroDyn for aerodynamics and a custom algorithm for hydrodynamic forces to make a coupled model of a wind turbine. This study focuses on the design aspect of the turbine and floater based on decay tests in the time domain. The model did not consider the drivetrain or control systems.
- (Uski et al. 2004) used ADAMS (MBS with AeroDYN) for the mechanics (blades, tower, drivetrain) combined with Matlab/Simulink models/codes for the control system and generator operations. Additional electrical components were modeled in PSCAS/EMTDC. The focus of this project was to provide a global approach to the wind turbine system. It is however unclear how the MBS model was set up and was only done for a fixed speed wind turbine.
- (Xie et al. 2020) developed a coupled model including gearbox dynamics coupled with BEM for aerodynamics and soil-structure interaction for a bottom fixed turbine. The results of this study are further discussed in the next Section.

One clear advantage of MBS modelling is the fast computation speeds when compared to FEM models but FEM models can achieve higher levels of accuracy for local stresses in materials (Christl et al. 2015). There are however some approaches that allow to combine the strengths of various methods such as gear meshing in SIMPACK as will be discussed in Section 3.7.

3.4 Aerodynamics

The aerodynamic interaction between the wind and the rotor is the underlying principle for the electricity production for any wind turbine. The additional degrees of freedom for a FOWT do however add to the complexity of these calculations. The aerodynamic module used in Simpack is "AeroDyn v. 15." and is based on the OpenFast code by (NREL 2020). The version used in this paper is based on the quasi-static BEM method as presented in Section 3.4.4.

3.4.1 Basic Aerodynamics

3.4.2 Momentum Theory

The most basic approach is to consider the turbine as an infinite disk in a one dimension ideal control volume (as shown in figure 11) and apply conservation of mass, momentum and Bernoulli's' equation on both sides of the pressure drop. The maximum power that can be extracted then becomes:

$$P_{max} = \frac{1}{2} C_p \rho A v_0^3 \quad (1)$$

$$C_P = 4a(1 - a)^2, a = \frac{v_0 - v_a}{v_0} \Rightarrow C_{P_{max}} = \frac{16}{27} \approx 59.3\% \quad (2)$$

Where; ρ is the density of the air, A is the rotor swept area, v_0 is the incoming wind speed, C_p the power coefficient and a the axial induction factor. The maximum power coefficient is called the Betz limit.

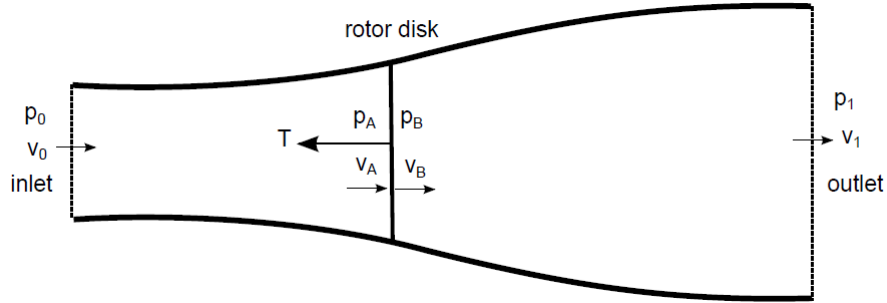


Figure 11: 1D Momentum Theory Diagram

3.4.3 Wake rotation

The torque exerted by the blades will cause the wake to rotate (eddies generation). By introducing a tangential induction factor:

$$a' = \frac{\omega}{2\Omega} \quad (3)$$

Where ω is the angular velocity of the free stream and Ω is the angular velocity of the rotor. The thrust and torque can then be calculated by integrating over an annulus (Δr) as shown in the figure below.

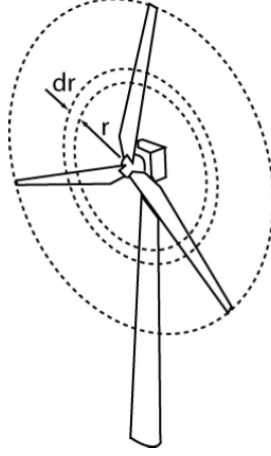


Figure 12: Annular Plane

The expressions used for thrust and torque, as well as the power obtained by the product of the torque and rotor angular velocity can be expressed as:

$$\Delta T_{MA} = 4a(1-a)\frac{1}{2}\rho v_0 2\pi r \Delta r \quad (4)$$

$$\Delta Q_{MA} = 4a'(1-a)\frac{1}{2}\rho v_0 \Omega 2\pi r \Delta r \quad (5)$$

$$\Delta P = \Omega dQ \quad (6)$$

We can also introduce another important parameter called the Tip Speed Ratio (TSR) as a function of the outer rotor radius R . As well as its local equivalent tsr .

$$TSR = \frac{R\Omega}{v_0} \quad (7)$$

$$tsr = \frac{r\Omega}{v_0} \quad (8)$$

3.4.4 Blade Element Momentum (BEM) Method

3.4.5 Background

The BEM method is based upon the momentum analysis for axial and tangential flow presented above combined with the aerodynamic behaviour of a finite number of blades. We can express lift and drag forces respectively as following:

$$\Delta \vec{L} = \frac{1}{2} C_l \rho \vec{V}^2 c \Delta r, \vec{L} \parallel \vec{V} \quad (9)$$

$$\Delta \vec{D} = \frac{1}{2} C_d \rho \vec{V}^2 c \Delta r, \vec{D} \perp \vec{V} \quad (10)$$

Where; Δr are span elements, c is the chord length of the blade element and \vec{V} is the incoming flow velocity. C_l and C_d are the lift and drag coefficients, they are a function of the angle of

attack α and the Reynolds number Re . Typically, their values are calculated from wind tunnel measurement or computations on 2D airfoils.

The inflow velocity (V_{Total}) will be a combination of the incoming wind, the rotor rotation and both axial and radial induction factors. The angle ϕ will be dependent on the angle of attack as well as the blade pitch angle. It is expressed as $\phi = \alpha + \beta$. This can be seen in Figures 13. Figure 14 shows the aerodynamic forces acting on the blade based on air friction and circulation.

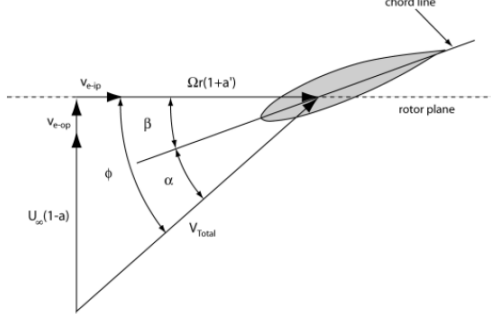


Figure 13: Blade Kinematics

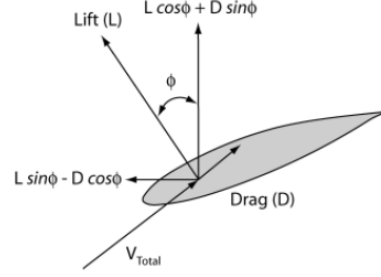


Figure 14: Blade Kinetics

Equations for thrust and torque can be written as following where the subscript BE stands for Blade Element. These will be dependent on the inflow angle ϕ expressed as a function of TSR and both axial and tangential induction factors.

$$\Delta T_{BE} = B(L\cos\phi + D\sin\phi)\Delta r \quad (11)$$

$$\Delta Q_{BE} = B(L\sin\phi - D\cos\phi)r\Delta r \quad (12)$$

$$\tan\phi = \frac{1 - a}{(1 + a')tsr} \quad (13)$$

A typical iterative algorithm as presented in (E. Bachynski 2020) can then be used to find a solution:

1. Guess starting values for a and a' .
2. Calculate ϕ and consequently α , C_l , and C_d .
3. Update a and a'
4. Check for convergence within a given tolerance, if not, repeat (starting from the updated values).

3.4.6 Correction Factors

Some engineering correction models are required to account for additional effects when using the BEM method. These are based on empirical or semi-empirical models. The equation in this section were taken from the theory manual for AeroDyn (Moriarty and Hansen 2005).

Firstly, there is a **tip loss effect** where the air tends to flow from the lower to the upper side of the blades around the tip based on the pressure gradient. This leads to a loss of aerodynamic forces. This is accounted by the Prandtl correction factor to the velocity field:

$$F = \frac{2}{\pi} \cos^{-1} \left[\exp \left(-\frac{B R - r}{2 r \sin\phi} \right) \right] \quad (14)$$

The second correction factor is related to the **hub-loss model**. This accounts for the vortexes being shed near the hub of the motor. It is implemented in the same manner as the tip-loss effect with the following formulation:

$$F = \frac{2}{\pi} \cos^{-1} \left[\exp \left(-\frac{B}{2} \frac{r - R_{hub}}{r \sin \phi} \right) \right] \quad (15)$$

The momentum method is not valid for axial induction factors superior to 0.5 (turbulent wake state). This would cause the far wake to have a negative velocity. The Glauert correction for **large induction factors** is therefore used to account for this as can be seen in Figure 15. It can be expressed as:

$$a = \frac{8}{9} + \left(4F - \frac{40}{9} \right) a + \left(\frac{50}{9} - 4F \right) a^2 \quad (16)$$

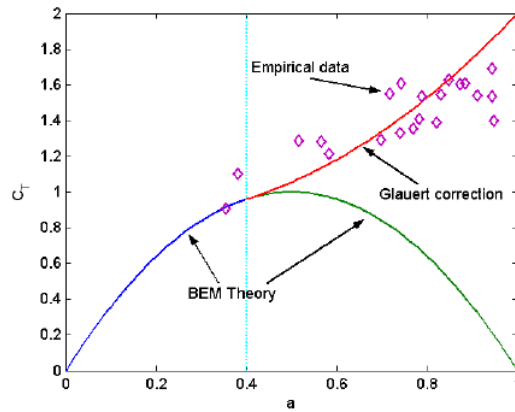


Figure 15: Glauert Correction for F=1

A **skewed wake** correction is implemented in Aerodyn as shown below to consider the effects of incoming flow that is not perpendicular to the rotor plane. Where, ψ is defined as the azimuth angle of the rotor based on tilt and yaw, and χ is the wake angle leaving the turbine.

$$a_{skew} = a \left[1 + \frac{15\pi}{32} \frac{r}{R} \tan \frac{\chi}{2} \cos \psi \right] \quad (17)$$

Dynamic stall, due to the sudden attachment and re-attachment of the flow on the blades for dynamic incoming wind, is accounted for using the Beddoes-Leishman model (Leishman and Beddoes 1989). It is based on an indicial response function to model the time variation in the force coefficients after a step change in angle of attack. It is a semi-empirical model for the circulatory component of the lift. In AeroDyn v.15, it is an Unsteady Aerodynamic (UA) model that accounts for these effects.

Dynamic wake is not currently supported by the Aerodyn BEM module. This correction accounts for the lag in induced velocities (mostly for high induction factors ie. low wind speeds). In addition, a Generalized Dynamic Wake (GDW) solver based on potential methods is also being developed (J. M. Jonkman et al. 2015). For large turbines it is advised to use the Free Vortex Wake (FVW) method named cOnvecting LAgragian Filaments (OLAF) which inherently models the effects of dynamic inflow skewed wake, tip losses and ground effects (NREL 2020).

3.4.7 Tower Influence

The tower will be exposed to the wind flow causing drag on the structure in addition to affecting the flow around the structure. This is important as the blades will pass through this field at 3-p frequency. In effect, the flow will tend to accelerate at the sides of the tower and cause cross stream velocities near the incoming flow field. A potential flow model is used to calculate the tower influence based on work from (Bak et al. 2001). The component affecting the blades is titled the upwind tower dam effect for an upwind turbine.

$$u = 1 - \frac{(x + 0.1)^2 - y^2}{((x + 0.1)^2 + y^2)^2} + \frac{C_d}{2\pi} \frac{x + 0.1}{(x + 0.1)^2 + y^2} \quad (18)$$

$$v = 2 \frac{(x + 0.1)y}{((x + 0.1)^2 + y^2)^2} + \frac{C_d}{2\pi} \frac{y}{(x + 0.1)^2 + y^2} \quad (19)$$

Where, u and v are horizontal wind velocity components in the x and y direction as shown in Figure 16 and C_d is the drag coefficient. This model

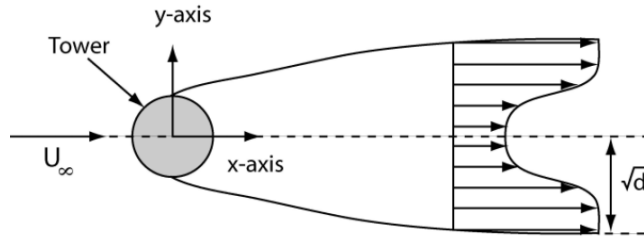


Figure 16: Tower Shadow

The aerodynamic load on the tower is calculated based on the drag forces dictated by the flow conditions and the geometry along the tower in a quasi-static calculation which is independent from the tower flow influence model presented above.

3.4.8 Wind Input

The wind input is crucial for the calculation of the aerodynamic forces. The wind data can be defined from simple "hub-height" wind files or from "full-field" files that contain turbulent components at points on a grid. Both cases are time-dependent and can be derived from simulations or measurements.

The "hub-height" wind files are defined by; hub-height wind speed and direction, vertical and horizontal wind shear coefficients, a vertical wind component, and a gust velocity. If the file has multiple data lines, linear interpolation in time is used.

Full-field wind data can be generated by the NREL TurbSim code (B. Jonkman and Jr 2007). It generates an array containing all three velocity components at each point on a square grid covering the rotor area and tower. These winds are typically sampled at 20 Hz. Again, linear interpolation in time and space is used to get the velocity components for the blade elements.

Various wind inputs can be used to simulate short term wind response for gusts and/or direction changes. Long term conditions can be represented by statistical distributions. This is typically used to determine which conditions most contribute to fatigue damage and power production.

3.4.9 AeroDyn in Simpack

In Simpack, the AeroDyn module labeled force element (237), it is based on the v1.0.0 version of OpenFAST. Some of the functionalities previously presented are for the latest version of OpenFAST and are therefore not guaranteed to be compatible within SIMPACK. AeroDyn is controlled by an input file that allows to choose between several options for induction and aerodynamic calculations as well as setting the environmental conditions the turbine operates in.

AeroDyn communicates the forces and torques acting on the rotorblades and tower to SIMPACK. These are applied at the aerodynamic markers defined during the model setup. These forces are based on the aerodynamic response to the wind file as described in the previous section. The communication interval between SIMPACK and AeroDyn is to be set as a discrete time step (Simpack 2020c).

The markers needed for the interface in Simpack are;

- Inertial Reference Marker: fixed with respect to the un-deflected tower center-line. xy plane is the water and z direction is vertically upwards. The X axis is downwind.
- Hub Markers: located on the hub body and rotates with the rotor
- Blade Root Markers: located on the blade bodies and pitches with the blades.
- Aerodynamic Marker: along the blades and tower required to design positions, velocities and orientations to AeroDyn.

3.4.10 Wind Turbine Control

A controller is required to ensure the wind turbine is operating at maximum efficiency below rated wind speed and at a constant torque thereafter. For larger turbines, this is achieved using blade pitch controller which adjust the pitch of the blades in order to control the output based on the aerodynamic behaviour of the blades. Such a system is also essential in order to park the turbine in winds outside of the design envelope. A typical graph showing various parameters is shown in Figure 17. As we can observe, the pitching is activated at rated wind speed (around 12 m/s), this causes the rotor speed and therefore power to be stabilized. The thrust which will cause surge and pitching of the platform is also shown in green.

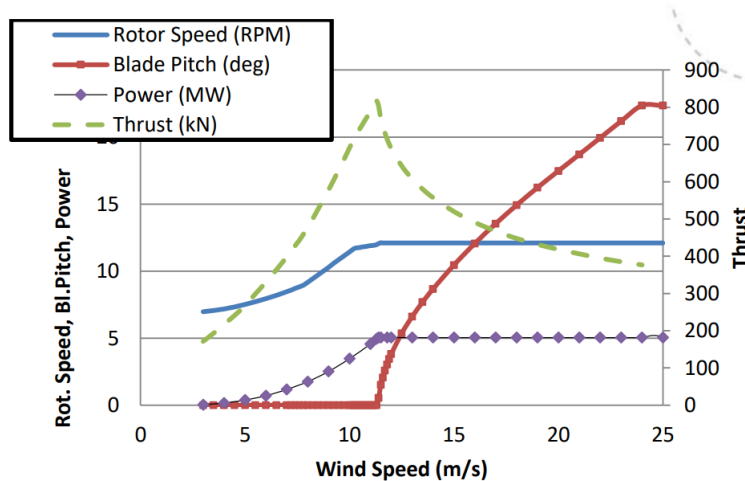


Figure 17: Typical FOWT Operation

In SIMPACK, the control system can be achieved by using a dedicated wind turbine control interface integrating standard Wind Turbine DLL's (ie. GH Bladed).

3.5 Rotor Blade Generation

The rotor blade generation is achieved by using standard input data common within the wind turbine industry. These specifications are then used by the SIMBEAM module that convert them to a flexible body (Simpack 2020c). We can see an example of this in Figure 21, the data provides the cross section of the blade at a given interval and SIMBEAM will generate the flexible beam elements between these nodes.

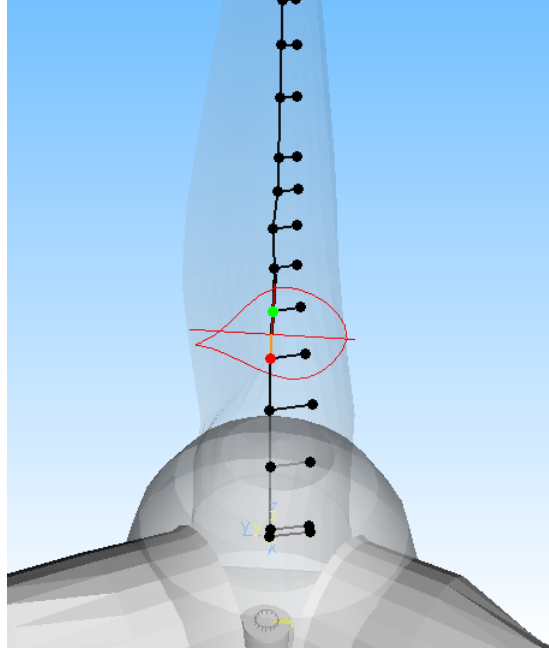


Figure 18: Rotorblade Generation in SIMPACK

3.6 Structural Mechanics

The wind turbine structure consists of a tower (attached to the platform), a nacelle, rotor and the blades. Modelling the loads on these components is essential to ensure that the turbine design is capable of sustaining structural loads during operation. These loads can be classified in several categories:

1. Accidental Limit State (ALS): The system shall withstand the maximum applied loads for a given design life in normal operation
2. Ultimate Limit State (ULS): In case of an abnormal event or extreme loading or fault case, the system shall not lose its integrity. For example, installing a weak link.
3. Fatigue Limit State (FLS): The system shall not fail under fatigue loadings in the design life

3.6.1 Flexible Bodies

The flexible bodies are generated using Finite Element Methods (FEM) allowing to include deformations of components. This is paramount for modelling the composite material wind turbine blades which experience significant deflections. A rigid body model does not provide enough information for structural strength analysis (Cruz and Acheson 2016). A general description of the structural dynamics equation for Finite Element Analysis (FEA) can be expressed as:

$$\mathbf{M}_g \ddot{\vec{D}} + \mathbf{B}_g \dot{\vec{D}} + \vec{R}^{int} = \vec{R}^{ext} \quad (20)$$

$$\vec{R}^{int} = \mathbf{K}_g \vec{D} \quad (21)$$

Where, \mathbf{M}_g is the element mass, \mathbf{B}_g is the damping matrix, \mathbf{K}_g is the stiffness matrix and \vec{D} is the system displacement vector. The stiffness matrix is not always linear due to geometrical nonlinearities (large deflections of the blades) and material nonlinearities. The element stiffness and mass matrices are defined based on the material properties.

FEM models can be generated internally in SIMPACK using the SIMBEAM module or imported from an external FEM software such as Abaqus (Simpack - Simulia 2020). As the name suggests, SIMBEAM is based on beam element theory. The finite elements can be of the various types as listed below.

- Rigid massless: only the kinematics of the element is applied
- Rigid with mass: with mass properties
- Euler-Bernoulli: Flexible beam element that does not include shear effects (underpredicts deflections and overpredicts eigenfrequencies)
- Timoshenko: Flexible beam element that includes shear strain and rotational inertia

Note that each node has 6 DOF and that the beams are always connected between two nodes.

If we define the dimensions of a beam: l is the length and d is a typical cross-section. Then the recommended flexible beam method can be defined as:

$$\frac{l}{d} > 10 \rightarrow Euler - Bernoulli, \quad (22)$$

$$10 > \frac{l}{d} > 5 \rightarrow Timoshenko \quad (23)$$

A modal representation of the beams is then derived from the FEM model, an example of the first mode of a flexible wind turbine blade is shown in Figure 26 with a scaling factor of 2 for visualization.

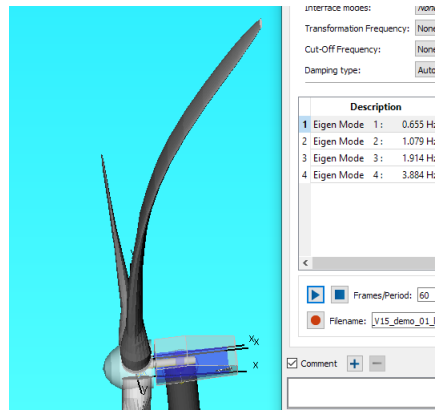


Figure 19: Blade Mode 1

The effect of the flexible bodies on the equations of motion is updated following the procedure shown in Figure 27. This mode shape approach is also used in the FAST code, it is a computationally efficient method with reasonable accuracy if the modes are well defined (Cruz and Atcheson 2016).

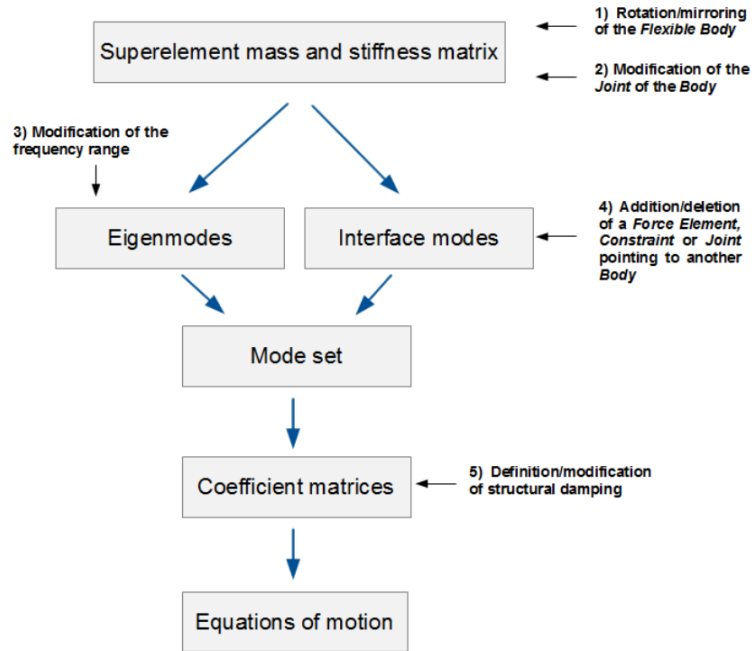


Figure 20: SIMPACK EOM Update Process (Simpack 2020e)

3.6.2 Structural Stresses

The structural calculations provide the forces acting on various parts of the system that can be used to derive the material stresses. The structural loads are a combination of static (gravity, buoyancy) and dynamic (wind, wave) loads. From time-varying analysis we can use stress cycle counting methods such as rain flow counting to determine the remaining life based on the Palmgren-Miner linear damage hypothesis (Veers 2011). The governing equations are:

$$N = K * S^{-m} \quad (24)$$

$$\sum_{i=1}^n \frac{n_i}{N_i} \leq 1 \quad (25)$$

Where, N is the number of cycles tolerated before failure, S is the stress range, and K and m are material properties from testing. $D = 1$ represents the failure of the component, n_i is the number of stress cycles associated with s_i and N_i is the number of cycles the material can tolerate at s_i . This would constitute the FLS assessment.

For the ULS, the stresses are calculated and compared to material properties under the most extreme operating conditions. If more detail is required for certain known weak links of the structure. A detailed FEA model can be set up in order to identify any stress concentration points such as welds or geometry changes.

3.6.3 Rotor Blade Generation

The rotor blade generation is achieved by using standard input data common within the wind turbine industry. These specifications are then used by the SIMBEAM module that convert them to a flexible body (Simpack 2020c). We can see an example of this in Figure 21, the data provides the cross section of the blade at a given interval and SIMBEAM will generate the flexible beam elements between these nodes.

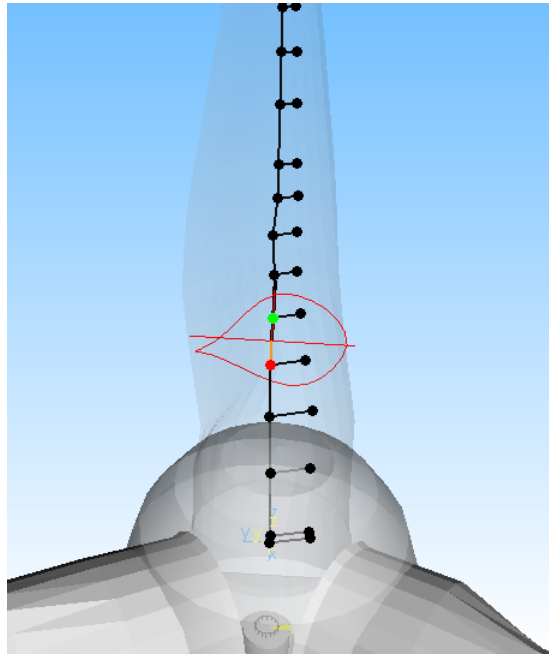


Figure 21: Rotorblade Generation in SIMPACK

3.7 Drivetrain Mechanics

The drivetrain of a wind turbine allows to transfer the kinetic wind energy to electrical power in the generator. It comprises all components such as: the shafts, gears, bearings, couplings and support structure present in the nacelle. The three main gearbox arrangements used today are:

3.7.1 Gearbox

- High speed gearboxes, these have gear ratios of around 1/100. This means that the output shaft angular velocity is 100 times larger than the rotor angular velocity. They represented the vast majority (85%) of drivetrain topology in 2011 (A. Ragheb and M. Ragheb 2010). A typical arrangement consists of 2 planetary gearbox stages and one parallel gear stage. The planetary gearboxes are widely used due to their compactness and price efficiency. The spur gears are easy to manufacture but can cause more noise pollution (Amir Rasekhi Nejad 2018).
- Direct drive, where the rotor is directly coupled to a large generator with numerous electromagnetic poles. The advantage of this design is the reduction of moving parts but can be more voluminous and heavy.
- Medium drive, a compromise between the two aforementioned options. The generator is made bigger but kept compact by the use of a gearbox with 1/10 ratio.

The power efficiency of the wind turbine gearbox can be estimated based on the power losses for planetary and parallel stages, respectively 1 and 2% (Hau 2006)

MBS software is well suited for the modelling of wind turbine drivetrains. In SIMPACK the gear bodies (rigid or flexible) can be generated based on their standard involute gear parameters through a dedicated gear modelling interface (body type 25). The contact force between the gears is then achieved through a dedicated force element (FE:225). For rigid bodies, the gears are coupled with a typical spring-damper combination to calculate the contact forces. A backlash element is put in series to the spring to account for the unilateral contact (Ziegler and Eberhard 2011). There are several additional options to model with flexible teeth and/or bodies (Simpack 2020a), this can for

example be used to represent flexible ring gears for load sharing (Stoekicht design). In addition to this, the number of degrees of freedom of the gear joints can be changed to model flexible planet gear pins (Hicks design) and floating sun gear designs.

An example of a MBS gearbox model made in SIMPACK for the 5MW NREL reference turbine is shown in Figure 22 (Amir Rasekhi Nejad, Guo et al. 2016). A similar model was also developed for the 10MW DTU reference turbine (S. Wang, Amir R Nejad and Torgeir Moan 2019). Another iteration of a reference gearbox was also modelled by (Xie et al. 2020), the associated gearbox topology is shown in Figure 23.

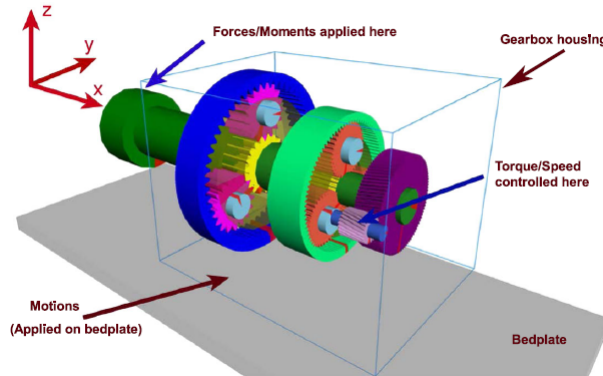


Figure 22: 5MW High Speed Gearbox MBS Model Graphical Representation

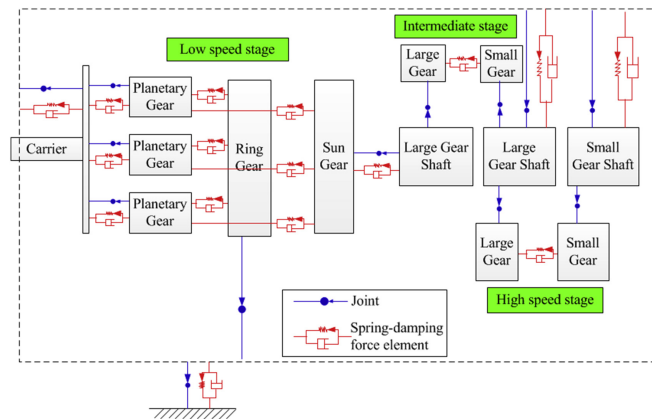


Figure 23: 5MW High Speed Gearbox MBS Model Topology

The simulation output forces acting on the gears can be used to derive the stresses acting on the gear teeth. The fatigue analysis is mostly focused on stresses acting at the teeth root and the surface pitting stress (Amir Rasekhi Nejad 2018). FEM methods can be used to determine the maximum stresses or empirical methods as described in ISO 6336-2 and 6336-3 respectively for pitting and tooth bending stress.

3.7.2 Bearings

The bearings can be represented by a force elements (FE:43) that provide stiffness and damping in specified directions. The force-deflection relationship in bearings was investigated by (Xing 2013) and is graphically shown in Figure 24. The use of expressions in SIMPACK allow to include these non-linear effects (Simpack 2020b). The stiffness parameters are input as shown in the matrix in Figure 25. The damping in rolling elements is usually negligible but necessary for the stability of the MBS model. Based on previous studies, values between 0.25 and 2.5% can be used to this effect (Krämer 1993).

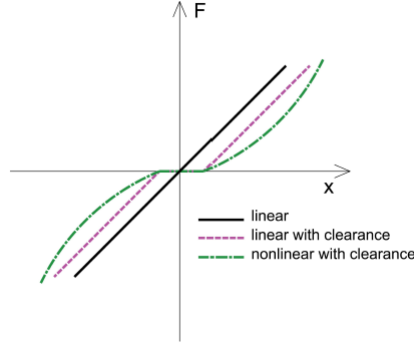


Figure 24: Force-deflection relation in bearings

$$\mathbf{K} = \begin{pmatrix} K_x & 0 & 0 & 0 & 0 & 0 \\ & K_y & 0 & 0 & 0 & 0 \\ & & K_z & 0 & 0 & 0 \\ & & & K_\alpha & 0 & 0 \\ sym. & & & & K_\beta & 0 \\ & & & & & K_\gamma \end{pmatrix}$$

Figure 25: Bearing Stiffness Matrix

By analysing the applied loads on these components, a fatigue analysis can be conducted based on empirical formulas developed by Lundberg and Palmgren in the 1960's. These are the equations used in the wind turbine standard IEC 61400-4.

$$L = \left(\frac{C}{P}\right)^a \quad (26)$$

$$P = XF_{radial} + YF_{axial} \quad (27)$$

Where, L is the bearing life which represents the number of cycles required for fatigue damage to appear for 90% of an identical group of bearings. C is the basic load rating and parameter a is set to 3 for ball bearings and $\frac{10}{3}$ for roller bearings. P is the dynamic equivalent radial load from the displacement in X and Y and corresponding forces.

3.7.3 Additional Considerations

Additional work on the model includes the assessment of a flexible bed-plate (S. Wang, Amir R Nejad, Erin E Bachynski et al. 2020) supporting the drivetrain for a FOWT. This study concluded that loads on bearings inside the gearbox were increased while the main bearing loads were decreased. It also showed that the bedplate flexibility makes the gearbox resonant response larger compared to a rigid bedplate.

Some geometrical imperfections related to manufacturing defects and tolerances can also be simulated. These can be classified in four categories: tooth profile deviations, backlash, misalignment and mesh phasing. These effects can be modelled in MBS software, where the effect with the highest defective impact was found to be misalignment which increases contact stress and/or cause edge contacts (Amir Rasekhi Nejad, Torgeir Moan et al. 2012). Having a flexible and floating sun gear can mitigate these misalignment issues and should be considered (Amir Rasekhi Nejad, Xing et al. 2015).

Lastly, the possibility of using land based wind turbine gearboxes in floating wind turbine should be considered. Studies on the 5MW reference turbine mentioned previously on a multitude

several type of platforms showed that the main bearing carrying axial loads experiences more damage in floating conditions. Other bearings were however found to perform equally or better than on land based conditions (Amir Rasekhi Nejad, Erin E. Bachynski et al. 2015).

3.8 Structural Mechanics

The wind turbine structure consists of a tower (attached to the platform), a nacelle, rotor and the blades. Modelling the loads on these components is essential to ensure that the turbine design is capable of sustaining structural loads during operation. These loads can be classified in several categories:

1. Accidental Limit State (ALS): The system shall withstand the maximum applied loads for a given design life in normal operation
2. Ultimate Limit State (ULS): In case of an abnormal event or extreme loading or fault case, the system shall not lose its integrity. For example, installing a weak link.
3. Fatigue Limit State (FLS): The system shall not fail under fatigue loadings in the design life

3.8.1 Flexible Bodies

The flexible bodies are generated using Finite Element Methods (FEM) allowing to include deformations of components. This is paramount for modelling the composite material wind turbine blades which experience significant deflections. A rigid body model does not provide enough information for structural strength analysis (Cruz and Atcheson 2016). A general description of the structural dynamics equation for Finite Element Analysis (FEA) can be expressed as:

$$\mathbf{M}_g \ddot{\vec{D}} + \mathbf{B}_g \dot{\vec{D}} + \vec{R}^{int} = \vec{R}^{ext} \quad (28)$$

$$\vec{R}^{int} = \mathbf{K}_g \vec{D} \quad (29)$$

Where, \mathbf{M}_g is the element mass, \mathbf{B}_g is the damping matrix, \mathbf{K}_g is the stiffness matrix and \vec{D} is the system displacement vector. The stiffness matrix is not always linear due to geometrical nonlinearities (large deflections of the blades) and material nonlinearities. The element stiffness and mass matrices are defined based on the material properties.

FEM models can be generated internally in SIMPACK using the SIMBEAM module or imported from an external FEM software such as Abaqus (Simpack - Simulia 2020). As the name suggests, SIMBEAM is based on beam element theory. The finite elements can be of the various types as listed below.

- Rigid massless: only the kinematics of the element is applied
- Rigid with mass: with mass properties
- Euler-Bernoulli: Flexible beam element that does not include shear effects (underpredicts deflections and overpredicts eigenfrequencies)
- Timoshenko: Flexible beam element that includes shear strain and rotational inertia

Note that each node has 6 DOF and that the beams are always connected between two nodes.

If we define the dimensions of a beam: l is the length and d is a typical cross-section. Then the recommended flexible beam method can be defined as:

$$\frac{l}{d} > 10 \rightarrow \text{Euler - Bernoulli}, \quad (30)$$

$$10 > \frac{l}{d} > 5 \rightarrow \text{Timoshenko} \quad (31)$$

A modal representation of the beams is then derived from the FEM model, an example of the first mode of a flexible wind turbine blade is shown in Figure 26 with a scaling factor of 2 for visualization.

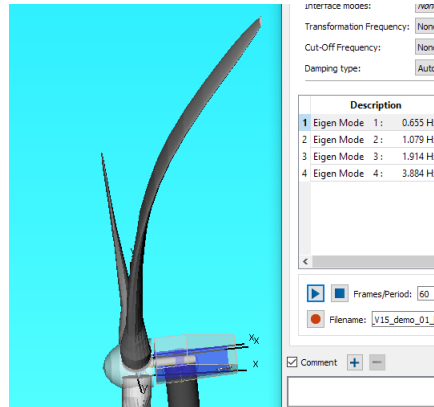


Figure 26: Blade Mode 1

The effect of the flexible bodies on the equations of motion is updated following the procedure shown in Figure 27. This mode shape approach is also used in the FAST code, it is a computationally efficient method with reasonable accuracy if the modes are well defined (Cruz and Atcheson 2016).

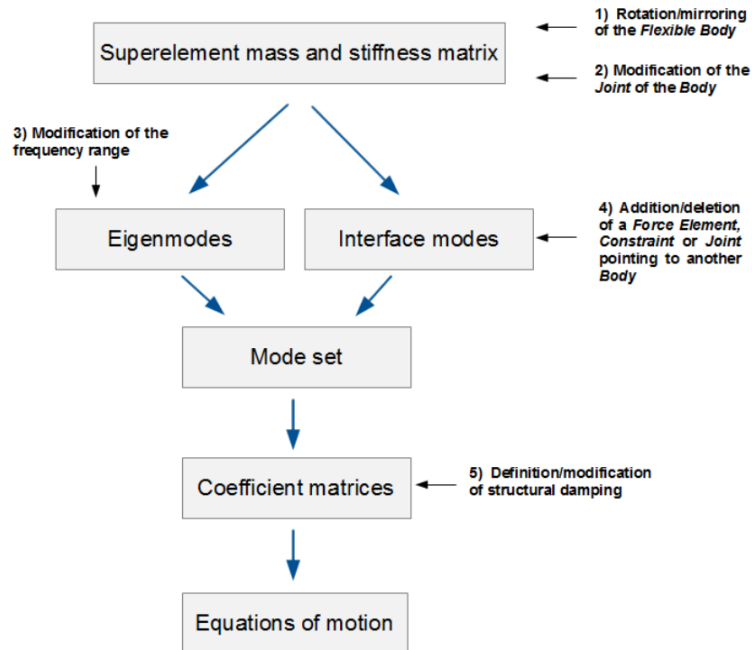


Figure 27: SIMPACK EOM Update Process (Simpack 2020e)

3.8.2 Structural Stresses

The structural calculations provide the forces acting on various parts of the system that can be used to derive the material stresses. The structural loads are a combination of static (gravity, buoyancy) and dynamic (wind, wave) loads. From time-varying analysis we can use stress cycle counting methods such as rain flow counting to determine the remaining life based on the Palmgren-Miner linear damage hypothesis (Veers 2011). The governing equations are:

$$N = K * S^{-m} \quad (32)$$

$$\sum_{i=1}^n \frac{n_i}{N_i} \leq 1 \quad (33)$$

Where, N is the number of cycles tolerated before failure, S is the stress range, and K and m are material properties from testing. $D = 1$ represents the failure of the component, n_i is the number of stress cycles associated with s_i and N_i is the number of cycles the material can tolerate at s_i . This would constitute the FLS assessment.

For the ULS, the stresses are calculated and compared to material properties under the most extreme operating conditions. If more detail is required for certain known weak links of the structure. A detailed FEA model can be set up in order to identify any stress concentration points such as welds or geometry changes.

3.9 Hydrodynamics

There are several considerations that need to be made when assessing the hydrodynamics of the FOWT system. Among these are station-keeping, stability, wave loads, current loads, damping.

3.9.1 Stability

The buoyancy was discovered by Archimedes. It says that there is a force balance between the structure weight and buoyancy force. When modelling the buoyancy of large volume structures it is calculated from the wet surface of the structure. This is done by the radiation/diffraction model.

3.9.2 Airy wave theory

Linear (or Airy) wave theory is the simplest wave theory for simulating linear regular wave. The elevation of linear regular wave surface can be shown as:

$$\eta_{LR}(t) = \frac{H}{2} \cos(kx - \omega t) \quad (34)$$

H is the wave height, k is the wave number and ω is the frequency of the wave.

The underlying principles of linear wave theory is (Cruz and Atcheson 2016):

- The free-surface and the body boundary conditions are linearised;
- The fluid is assumed incompressible and the flow is irrotational;
- Viscous effects like flow separation and shear stresses are not considered;
- The bottom is uniform and flat;

3.9.3 Potential-flow theory

Potential theory models are suitable for large volume models. The floater is modelled as a three-dimensional diffracting body. To calculate the wave loads on the body a panel method is used. The use of at least 7-10 panels per wavelength is suggested. Potential flow panel models enables investigation of diffraction and radiation forces. To include viscous damping and viscous forces parts of Morison equation may be adopted. By assuming an equilibrium position for the floater and a harmonic solution to the velocity potential the first-order-quantities can be derived.

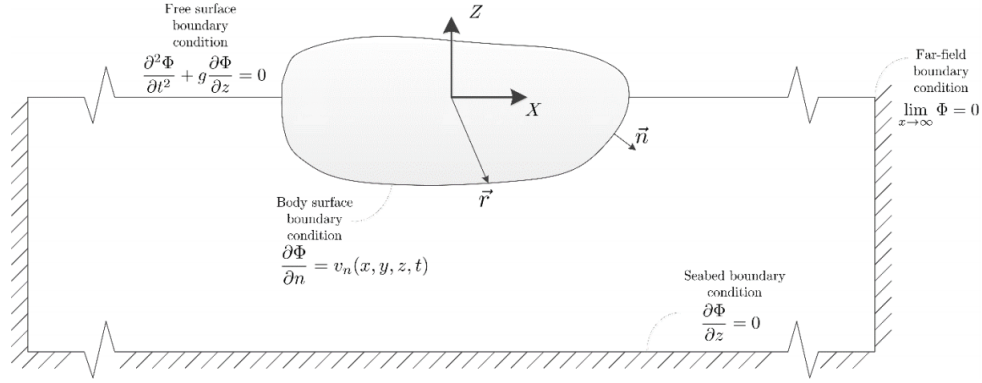


Figure 28: Boundary conditions for the linearized potential flow problem (Borg and Bredmose 2015)

$$\Phi(x, y, z) = \Phi_w + \Phi_d + \Phi_r \quad (35)$$

$$\nabla^2 \Phi = 0 \quad (36)$$

$\Phi(x, y, z)$ is the velocity potential. Φ_w represents the incident wave field, Φ_d represents the diffracted wave field and Φ_r represents the radiated wave field. The Laplace equation given in the formula above is applied to establish the velocity potential and the surface pressure of the body. The global force \vec{F} and moment \vec{S} contributions can be computed.

$$\vec{F} = \rho_w \int \int_S \left(\frac{\partial \Phi}{\partial t} + gz \right) \vec{n} \cdot dS \quad (37)$$

$$\vec{M} = \rho_w \int \int_S \left(\frac{\partial \Phi}{\partial t} + gz \right) (\vec{r} \cdot \vec{n}) \cdot dS \quad (38)$$

Wetted surface of structure in equilibrium position is represented by S , g is acceleration due to gravity, \vec{n} is the body surface normal vector, z is the vertical coordinate from mean sea level and \vec{r} is the corresponding distance vector from coordinate system origin. To apply the results in time-domain Cummins equation is used (Borg and Bredmose 2015).

3.9.4 Morison

Morison's equation is valid for slender cylinders and is a function of the diameter, fluid particle velocity and acceleration and the hydrodynamic drag and inertia coefficients C_D and C_M . The coefficients are functions of Reynolds number, keulegan-Carpenter number and surface roughness.

Hydrodynamic loads for slender structures can normally be modelled by using Morison formula (T. Moan et al. 2019).

$$F = \frac{1}{2}\rho DC_d\nu|\nu| + \frac{1}{4}\rho D^2 C_m a \quad (39)$$

Which expresses the lateral force per unit length on a slender member with a diameter D and particle velocities and accelerations of ν and a , respectively. C_d and C_m are drag and inertia coefficients, ρ is the water density. To calculate the loads on large volume structures potential theory, considering the incoming and diffracted wave pattern should be used. The hydrodynamic loads on floating structures need to be estimated by. Both the first- and second-order wave loads according to potential theory need to be considered, implying difference- and sum-frequency effects. In the linear analysis, both the diffraction and radiation effects are addressed, which results in the wave excitation forces and the added mass and the potential damping forces. Normally the viscous effects are modelled as drag forces and added to the potential forces (T. Moan et al. 2019). Zhang and Ishihara 2016 used an improved Morison equation to analyse a floating wind turbine.

Ramachandran et al. 2013 shows the typical ranges of natural periods for the different types of floating foundations. (T. Moan et al. 2019) shows the indicative natural frequencies and natural periods of "rigid body motion modes" of FOWTs. They find that the first bending mode of the tower coupled to a floating platform will be coupled to the platforms pitch and surge motions. T. Moan et al. 2019 finds that the the lowest frequency of rotation no longer is the first bending mode, but a rigid body pitch mode. They find that this pushes the first bending natural frequency higher and may therefore require changes in the design in order to avoid the tower resonance being excited by loads related to blade passing. They conclude that the drivetrain responses can be determined in an uncoupled manner because the natural frequencies of the drivetrain between the generator and rotor are much higher than the blade modes and rigid and flexible structure.

When applying Morison's equation by the means of strip theory there are several limitations. By using strip theory wave radiation damping is neglected. The wave loads include drag and an inertia term. Other limitations to strip theory is listed below.

- Simplification of diffraction problem
- Some of the terms of the added mass matrix are disregarded
- Hydrodynamic interaction between bodies is neglected
- Mostly devoted to simple geometries such as cylinders

3.9.5 Wave spectrum

To calculate the motions of the floating wind turbine, irregular wave loads are considered. The most common way to represent the sea state is by a wave spectrum. Typically Pierson-Moskowitz spectrum and JONSWAP spectrum are applied (Jahangiri and Sun 2019). For computational reasons spreading functions are ignored. It is assumed that waves travel in the same main direction. The equation below is of the JONSWAP spectrum. Several versions of the equation can be found in (Zuo et al. 2018), (Lemmer et al. 2020).

$$S_{JS}(f) = \alpha_2 H_S^2 T_P \left(\frac{f}{f_P} \right)^{-5} e^{-1.25(f/f_P)^{-4}} \cdot \gamma^\beta \quad (40)$$

Where f is wave frequency, T_P is peak wave period and H_S is significant wave height, $f_P = 1/T_P$, α_2 and β given by the IEC 61400-3 (Ghassempour et al. 2019):

$$\gamma = \begin{cases} 5 & T_P/\sqrt{H_S} \leq 3.6 \\ e^{5.57-1.15T_P/\sqrt{H_S}} & 3.6 \leq T_P/\sqrt{H_S} \leq 5 \\ 1 & T_P/\sqrt{H_S} \geq 5 \end{cases} \quad (41)$$

Where the coefficients are calculated from the formulas below.

$$\begin{aligned}\alpha_2 &= \frac{0.0624}{0.230+0.0336\gamma-0.185/(1.9+\gamma)}; \\ \beta &= \exp\left[-\frac{0.5}{\delta^2}\left(\frac{f}{f_P}-1\right)^2\right]; \\ \delta &= \begin{cases} 0.07 & f \leq f_P \\ 0.09 & f > f_P \end{cases}\end{aligned}\quad (42)$$

The waves that are included are 1st and 2nd order. The second order waves are in some cases included in potential wave theory models. Currents may also be of importance when modeling the floater and mooring lines. However the associated forces are usually assumed to be negligible.

Tide level may be of importance as it may affect the mooring system. The tension in the mooring lines may vary when using taut mooring. This is especially important for TLPs, but is often ignored for the other mooring systems. Because the coupling between the turbine forces and floater motions is strong the aerodynamic inflow conditions are influenced.

3.9.6 Wave frequency loads

The hydrodynamic loads can be divided into a viscous part and a non-viscous part. The linear part is often limited to drag while the non-linear part includes Froude-Krylov and diffraction terms. There are several theories that may be applied when modelling the loads on the floating substructure, diffraction/radiation and strip theories being the most common. The analysis is often done in time-domain, because it enables to capture the non-linear effects. Each part of the submerged structure should be modelled properly to give a correct analysis.

3.9.7 Damping

In the analysis of a FOWT the damping of all relevant components should be included. The sum of the individual components gives the total damping.

$$\zeta = \zeta_{struct} + \zeta_{hydro} + \zeta_{mooring} + \zeta_{soil} + \zeta_{aero} \quad (43)$$

The damping is given as damping ratio ζ or logarithmic decrement δ .

$$\zeta = \frac{d}{d_{crit}} = \frac{d}{2\sqrt{cm}} \quad (44)$$

$$\delta = \frac{2\pi\zeta}{\sqrt{1-\zeta^2}} \approx 2\pi\zeta \quad (45)$$

The formulas are for a single DOF system. d is damping, d_{crit} is critical damping, c is stiffness and m is mass.

3.9.8 Modelling Codes With Respect to Hydrodynamics

SESAM is a numerical tool for structural analysis of floating offshore turbine structures. It consists several modules. Some of these include Reflex, SIMA and SIMO. Further description of Sima and below.

SIMA is for efficient analysis of complex multi-body systems, including mooring analysis. Analysis including coupled effect of waves, wind and current for structural analysis or mooring can be performed. This combined effect must be taken into account. Some of the key benefits of Sima software as listed on dnv:

- Slender structure modelling of mooring lines.
- Choose between fully dynamic and simplified catenary model for mooring lines.
- Include any number of separate bodies in the simulation
- Hydrodynamic coefficients read in from HydroD.
- Time domain dynamic analysis with time series output of results.
- Regular or irregular waves with current, swell and wind.
- Static analysis and calculation of line forces/moments, curvature and displacements.
- 3D animation of vessel and line displacements.
- Data export to Sesam structural analysis modules for detailed finite element analysis of floater.

To perform analysis of floating offshore wind turbines the software has been extended with new features including:

- Wind load models.
- The wind turbine blades and tower can be flexible.
- Modelling of offshore wind turbine blades.
- Wind turbine modelling, including control system.

SIMO is for complex multi-body calculations. It can be used for all of the floating foundation designs and includes flexible modelling of stations-keeping forces and connecting force mechanisms(anchor lines, ropes, thrusters, fenders, bumpers, docking guide piles). Reflex is a riser analysis software. Modelling of Wind turbine drivetrain is however not included in any of the modules. Other examples of common numerical tools are represented in figure 29 below. (DNV-GL 2019)

<i>Software</i>	<i>Aerodynamics</i>	<i>Hydrodynamics</i>	<i>Structural dynamics</i>	<i>Mooring line dynamics</i>	<i>Controller modelling</i>
WAMIT	N/A	FD PT or TD CE	RB or Modal	GSM	N/A
AQWA	N/A	FD PT or TD CE + MD	RB or FEM (TD)	GSM or QSM or FEM	N/A
WINDOPT	N/A	FD PT	RB	QSM or FEM	N/A
FAST	(BEM or GDW) + DS or CFD	TD ME or CE + MD	Modal or MBS	GSM or QSM or FEM	DLL or UD or SM
BLADED	(BEM or GDW) + DS	TD ME or CE + MD	Modal or FEM	GSM or QSM or FEM or MBS	DLL
OrcaFlex	Coupled to FAST	TD ME or CE + MD	Coupled to FAST	GSM or QSM or FEM	Coupled to FAST
3DFloat	BEM	TD ME or CE + MD	FEM	GSM or FEM	DLL or UD
Flex5	BEM + DS	TD ME or CE + MB	FEM/modal	QSM	UD
HAWC2	(BEM or GDW) + DS	TD ME or CE + MD	MBS/FEM	GSM or QSM or FEM	DLL or UD
SIMA (SIMO/RIFLEX)	BEM + DS	TD ME or CE + MD	MBS/FEM	GSM or QSM or FEM	DLL or UD
Sesam/Wadam	N/A	FD PT + ME	RB	GSM	N/A
Simpack	(BEM or GDW) + DS or FVM or CFD	TD ME or CE + MD	MBS	GSM or QSM or MBS	DLL
SLOW	ACP	Reduced CE or ME	Modal or MBS	GSM or QSM	SM

Figure 29: Example of numerical tools (DNV-GL 2019)

Software	Aerodynamics	Hydrodynamics	Structural dynamics	Mooring line dynamics	Controller modelling
	<i>Aerodynamics</i> BEM - blade element momentum GDW - generalised dynamic wake DS - dynamic stall CFD - computational fluid dynamics FVM - free-wake vortex model ACP - actuator point model. <i>Hydrodynamics</i> FD - frequency domain TD - time domain PT - potential flow CE - Cummins equation MD - Morison drag term ME - Morison equation.		<i>Structural and mooring line dynamics</i> RB - rigid body MBS - multi-body system formulation FEM - finite element method GSM - global stiffness model QSM - quasi-static model. <i>Controller modelling</i> DLL - dynamic link library UD - user defined SM - Simulink-MATLAB interface.		

Figure 30: Example of numerical tools(continued). (DNV-GL 2019)

SIMA (SIMO/RIFLEX) is a numerical tool developed by MARINTEK and licenced by DNV GL. For large-volume hydrodynamic calculations SIMO-bodies are employed. A combination of frequency-domain potential flow data and distributed Morison elements are used. RIFLEX computes the structural response to all input loads using a finite element approach. 2^{nd} order wave loading is also included. Jiang et al. 2020 applied this software to analyse two spar type floating foundations designed to support 10MW wind turbines.

3.9.9 Modeling of floater

As mentioned above there are three ways to model the floater.

- Rigid body models is acceptable if the structural deformations do not contribute significantly to the global displacement of the FOWT. The floater is represented as a 6 DOF system. Flexibility of the model is more important when performing second order wave force calculations. This is especially valid when modelling TLPs as the system natural frequencies may be influenced by the platform flexibility (Ramachandran et al. 2013).
- Modal models are normally used in combination with a multi-body model. This is to include the contribution of mass, damping and restoring forces from hydro-elastic effects.
- Finite element and multi-body models are recommended if deformation of the floater is important. Flexible models are important for slender structures. The whole floater may be modelled as flexible or only parts in combination with one of the two other methods. An example of this can be seen in one of the examples available in SIMPACK. The example is a floating semi-submersible with three pontoons. The pontoons are modelled as rigid, while the beams connecting the pipes are modelled as flexible.

The floater is often modelled as rigid, but there are also work in the literature where the floater has been modelled as a flexible body (Lemmer et al. 2020). It is shown in (Zuo et al. 2018) that the worst case is the misalignment of 90degrees between wind and wave because of the loss of aerodynamic damping.

3.9.10 SIMPACK

The calculation of hydrodynamic loads is based on combination of 3-D linear potential flow theory and Morison's equation. The HydroDyn force element is labled force element 244. It is a multi-force

element, and integrates the software HydroDyn into Simpack.

The load includes contributions from linear hydrostatic restoring, non-linear viscous drag contributions from Morison's equation, added mass damping contributions from linear wave radiation and incident wave excitation from linear diffraction.

HydroDyn is a load calculation module that is used in SIMPACK. It is based on classical linearization theory in hydrodynamics, and calculates the response of the FOWT and the force on the mooring system in time-domain. To establish the hydrodynamic model using the potential flow the Airy Wave theory is used. This implies that the nonlinear viscous damping is ignored.

When modeling a floating system, one may use potential-flow theory only, strip-theory (Morison) only or a hybrid model containing both (NREL 2020). The floater may be modelled as either rigid, which is suitable for floaters with small flexibility, modal or FEM beam. Modal and FEM is suitable for slender floaters.

To include current loads HydroDyn it is required to use strip-theory only or a hybrid approach. The reason is that current is not used in the potential-flow solution, but includes the loads using strip- theory through drag terms. (NREL 2020).

A floating wind turbine has six degrees of freedom. There are three translational (surge, sway, heave) and three rotational (roll, pitch, yaw) motions.

- Surge is translation along the longitudinal axis
- Sway is translation along the lateral axis
- Heave is translation along the vertical axis
- Roll is rotation about the longitudinal axis
- Pitch is rotation about the lateral axis
- Yaw is rotation about the vertical axis

These degrees of freedom are presented in the following figure.

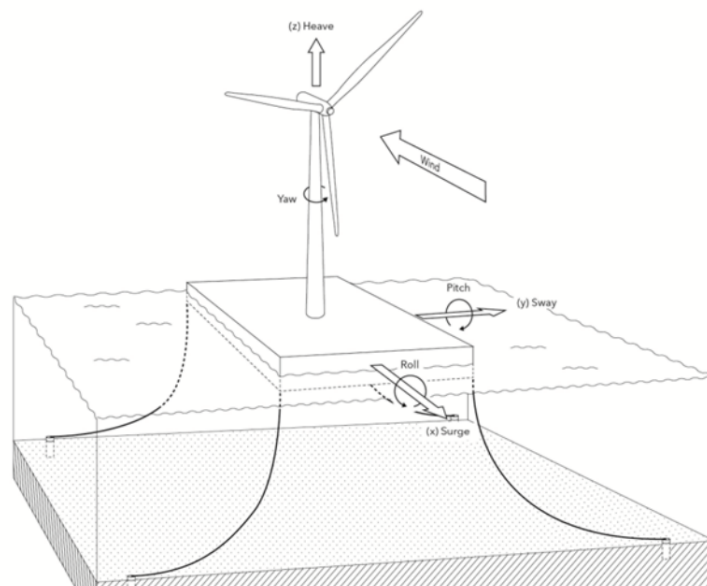


Figure 31: DOFs of a floating wind turbine. (Ramachandran et al. 2013)

3.10 Mooring System Modelling

Two alternatives exist when modelling mooring lines in a numerical analysis. These alternatives are commonly known as quasi-static or dynamic modelling. Quasi-static analysis refers to a mooring system which is modelled as linear or nonlinear springs. It is computationally efficient, but dynamic effects are not considered (Azcona et al. 2017). Inertia, added mass or drag forces produced by currents, waves or movement of lines is not included. These effects are considered in the dynamic models, but comes at the cost of higher computational effort. There exist some studies which compare the quasi-static model with the dynamic model. Some of these can be found in Azcona et al. 2017. For a taut system, the restoring force from the line is related to elastic deformation of the line and shows a linear behaviour. A catenary system gets restoring forces from the vertical-lift-off of the mooring line from the seabed and has by definition a non-linear relationship between top displacement and force. In a dynamic analysis the lines are modelled as slender elements, which enables including the mass and drag forces acting along the length of the line. The Quasi-static mooring line model is often sufficient for global analysis of the FOWT, but often underpredicts the mooring line tensions. A dynamic mooring line model should therefore be chosen. The choice of material can also influence the choice of chosen approach. (Borg and Bredmose 2015) discusses a number of methods for modelling mooring lines and concludes that the best method when carrying out design and optimizing beyond preliminary system sizing is dynamic mooring line models. Dynamic effects are typically more important for catenary systems in deep waters. Mooring line eigenmodes may occur, thus it is important that the damping is correctly represented in the model. Azcona et al. 2017 also reviewed and tested the the two alternatives for three types of floating platforms supporting a 5 MW wind turbine in water depth of 200m. For the dynamic approach they used the OPASS dynamic model, which is a lumped mass model for non-linear mooring dynamics. The model considers hydrodynamic added mass, gravity, wave kinematics, inertia, hydrostatics, line-seabed contact and friction, axial elasticity, structural damping and tangential and normal hydrodynamic drag. Descriptions and references to finding parameters, drag coefficients and added mass for the three floating foundations based on the main parameters of the floater are given in the work.

In the MBS approach the line is discretized into separate rigid or flexible bodies connected by spring-damper elements. The hydrodynamic forces on each element are calculated using Morison's equation.

When modelling mooring lines there are three options given in (Ramachandran et al. 2013) and listed below.

- 1: linear spring, which is a suitable option for floater motion analysis for floater using taut mooring;
- 2: non-linear spring, which is suitable for floater motion analysis for floater using catenary mooring;
- 3: multibody/FEM bar, which is more complicated.

Option 1 and 2 is not suitable for mooring design, but the third option is suitable for design. When using this option the FEM bar only has axial DOF. Fig 33 shows the mooring line topology with 3 mooring lines. Fig 32 shows the schematic diagram of the MBS mooring line model. The line consists of rigid bodies, but may also be modelled as flexible.

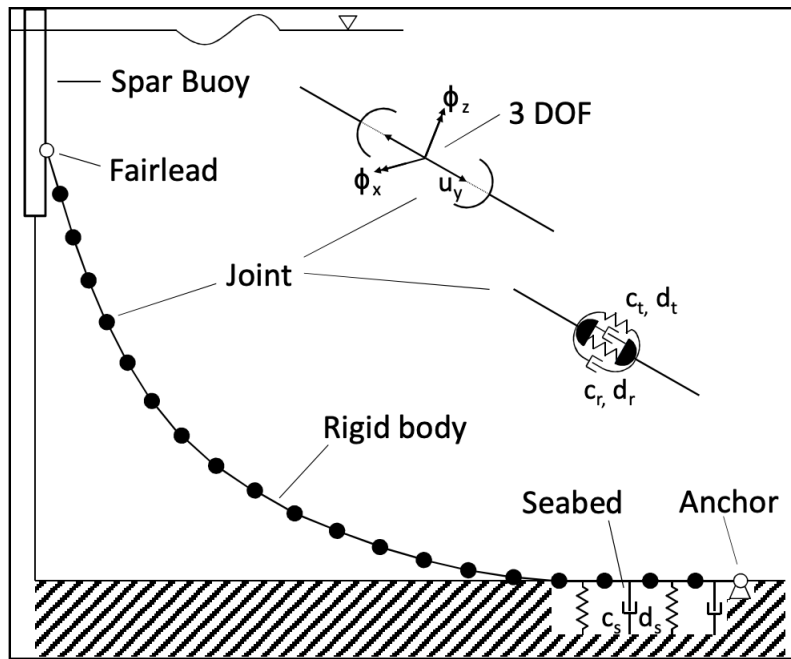


Figure 32: Schematic diagram of the MBS mooring line model ('Offshore Wind Turbine Hydrodynamics Modeling in SIMPACK' 2013), (Azcone et al. 2013)

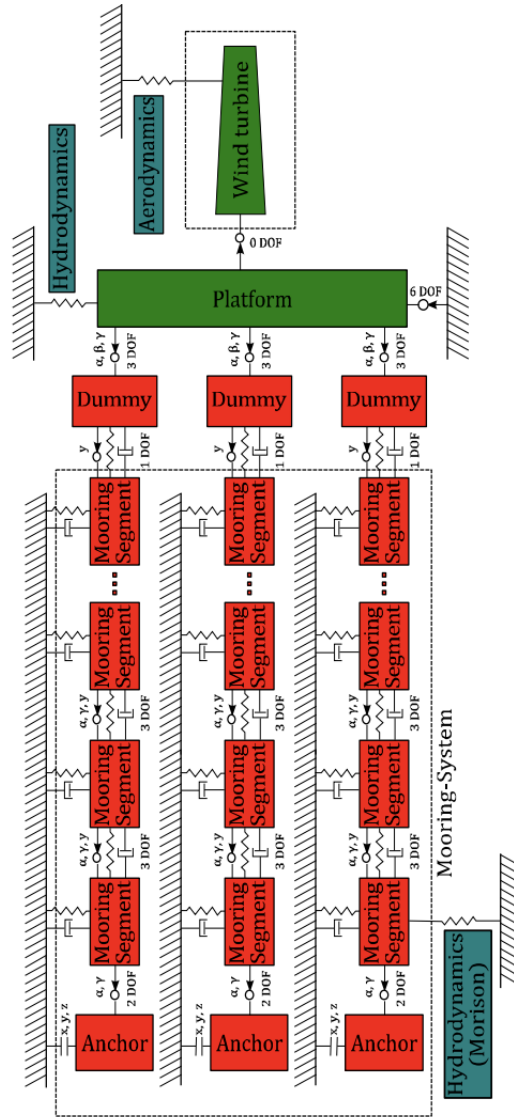


Figure 33: MBS mooring line topology (Azcone et al. 2013).

For further research on mooring systems the book "Mooring system engineering for offshore structures" (Ma et al. 2019) chapter 2,4,5,8 and 15 should be studied. NREL's MoorDyn should also be researched. Several other articles found in the literature review will also be further researched.

3.10.1 SSI Modelling for bottom-fixed foundations

Several articles have been published on work done to create models including SSI. There is a wide range of approaches, simplifications and software used to simulate the structural dynamics, soil and coupling between them. The Winkler method was first introduced. It uses p-y curves to model the interaction.

Zuo et al. 2018 modelled the part of the tower in the soil by using beam elements. They adopted non-linear soil springs to consider SSI. In this method, the lateral resistances of the soil against the pile movements are expressed by springs parallel and perpendicular directions of the rotor plane. t-z springs are applied vertically to simulate shaft friction, and a Q-z spring simulate the end bearing capacity. The p-y springs were placed with 1 m spacing. See figure 34.

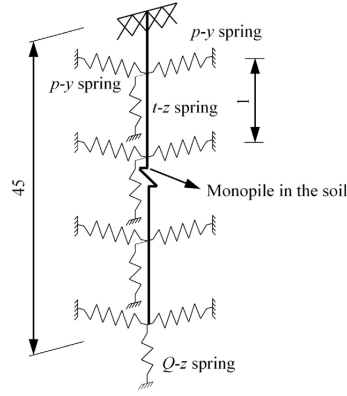


Figure 34: SSI modelling of monopile in soil (Zuo et al. 2018)

(Fitzgerald and Basu 2016) created three-dimensional models of the wind turbine foundation which were analysed in the finite element geotechnical code Plaxis. To describe the soil-structure interaction they used rotational springs with spring constants calculated by analysing the bi-axial rotations of the foundation. The authors used both dense sand and consolidated clay in their analysis and compared the results to NREL's aero-elastic model FAST.

(Carswell et al. 2015) presents a method for converting hysteric energy loss into a viscous, rotational mudline dashpot that represents OWT monopile foundation damping for a lumped parameter model.

(Cao et al. 2020) analysed an offshore monopile wind turbine using a new finite element method. The research discussed and compared the dynamic responses between the OWT model including soil-structure interaction using both traditional p-y method and the new model. They found that the traditional p-y method overestimates the displacements of the OWT under stochastic wave and wind loads. The most unfavorable situation was the combination of 90 degrees wind-wave angle and operating condition.

Most literature focuses on unidirectional response (fore-aft motion) mitigation while the real offshore wind turbines suffers from bi-directional vibration (fore-aft and side-side) due to wind-wave misalignment (Sun and Jahangiri 2018). By simplifying the foundation model in the xz and yz planes, the soil effects are considered and represented by rotational spring with coefficients $k_{x\phi}$ and $k_{y\phi}$ and translational springs with coefficient k_x and k_y . By introducing translational and rotational dampers with coefficients c_x , c_y , $c_{x\phi}$ and $c_{y\phi}$ the soil's damping property is considered (Sun and Jahangiri 2018). This is represented in figure 35. q_9 , q_{10} , q_{11} , q_{12} denote the translation and rotation coordinates of the foundation.

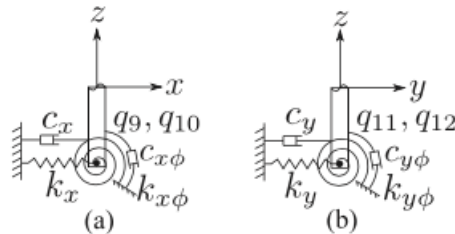


Figure 35: Simplified foundation model of offshore monopile wind turbine in xz and xy planes (Sun and Jahangiri 2018)

(Sun and Jahangiri 2018) used this method to analyse NREL 5MW OC3 monopile wind turbine and calculated the soil effect parameters using linear springs and dash-pots. To represent clay soil conditions the value of parameters $k_x, k_y, k_{x\phi}$ were obtained as $k_x = k_y = 3.89E9$ N/m, $k_{x\phi} = k_{y\phi}$

$= 1.14E11$ Nm/rad. The damping properties c_x , c_y , $c_{x\phi}$ and $c_{y\phi}$ were selected such that the corresponding damping ratio was 0.6 (Sun and Jahangiri 2018) based on (Carswell et al. 2015). (Xie et al. 2020) also used this method in their work.

(Carswell et al. 2015) gives an overview of work done on including soil effects in the analysis of offshore monopile turbines. Different methods and soil parameters are included. The work includes instruction on how to calculate parameters for foundation damping and stiffness using a lumped parameter foundation model.

(Gonzalez 2016) also modelled fixed foundation offshore wind turbines and presents a thorough review of theory and methods for modelling. The monopile is modelled by using lumped mass model, which simplifies the soil-structure interaction by a series of springs and dampers. See figure below.

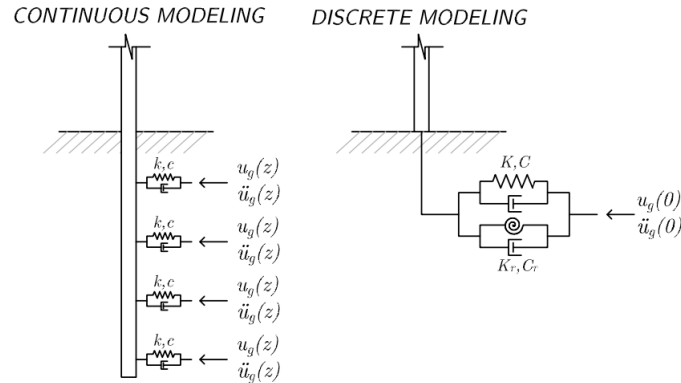


Figure 36: Continuous vs. Discrete modeling of soil. (Gonzalez 2016)

3.10.2 Soil Properties

There are several ways to represent the soil in the model. Simplifications are often used as the soil layering can be complex resulting in complex modeling. The soil is often defined in layers, with varying properties. These properties may be of interest if the soil has ads damping to the structure subjected to environmental loads. This impact will also be discussed for FOWT anchoring systems. For the North Sea, a simplified, but representative offshore soil profile is represented in figure 37.

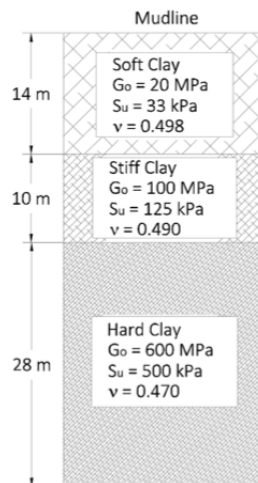


Figure 37: Representative North Sea offshore soil profile. (Carswell et al. 2015)

3.10.3 Soil-Structure Interaction

This section briefly presents some methods for modelling Soil-structure interaction (SSI) in case of fixed foundations. Parameters for characterizing the soil are discussed, and literature for further investigation is presented. Variations of floating foundations are briefly presented, followed by an introduction of the mooring system components and design variations. Modelling of the mooring system including SSI is then presented.

When a structure is in contact with the ground the displacement of the ground and structure are not independent of each other. The process by which the response of the underlying soil and the structural response affects each other is known as Soil-Structure Interaction (SSI) (Fitzgerald and Basu 2016). Traditionally, the wind turbine foundations were often modelled as fully fixed. With this simplification SSI is not considered. This may result in inaccurate modal parameters when analysing the system. Accounting for a flexible soil-foundation system can have the effect of reducing a wind turbine's fundamental natural frequency and introduces a considerable amount of damping to the system (Veletsos AS. and Verbic 1973). (Xie et al. 2020) also emphasises the importance of considering the effect of soil-structure interaction due to the reasons mentioned above. Several methods for analysing the soil-pile interaction are available, among these are analytical linear, viscoelastic continuum models, linear Winkler type medium models and finite-element models (Banerjee et al. 2019). Offshore wind turbines (OWT) are today mainly placed on fixed foundations, which can be seen in 5. Designing the foundation correctly, including all components and environmental loads has proved difficult. Inclusion of SSI is also important for operation of the OWT because of the blade passing. The blade passing will be further discussed later in this chapter. For floating offshore wind turbines (FOWT), the importance varies depending on the chosen mooring system. For catenary mooring the damping caused by the SSI is negligible, but for taut mooring used in mooring systems for TLPs the SSI can affect the global stiffness and damping.

3.10.4 Seabed Modelling

The interaction between the seabed and catenary system may be modelled as vertical seabed stiffness and lateral friction. To represent the seabed interaction effect in a mooring line being cyclically lifted on and off the seabed a non-linear analysis is needed. Soil information is used to decide the seabed stiffness and friction coefficients (Ramachandran et al. 2013). Elasticity of the mooring line may be influenced by the horizontal friction model, thus an incorrect friction model may result in low line tensions. When modelling the mooring system the anchor is often modelled as a fixed point. According to cite (DNV-GL 2019) this is often sufficient, however it is insufficient for taut mooring systems or a TLP as the soil may contribute to significant damping. The cable-seabed contact is modelled as seen in fig 38

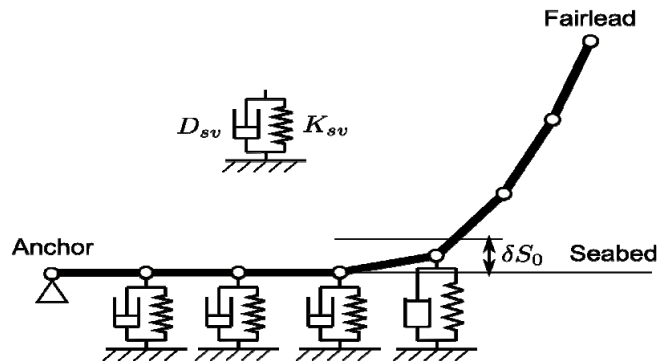


Figure 38: Cable-seabed contact model (Azcone et al. 2013).

3.10.5 SSI Modelling

There are multiple ways soil-structure interactions can be modelled in a fully coupled multi-body simulation. The soil-structure interactions were often ignored when modeling both land-based and offshore wind turbines. Work done by (Zuo et al. 2018) showed the importance of including SSI in the modeling because of the effect the interaction has on the structure. (Carswell et al. 2015) showed that by including SSI in the full-body model the total damping and natural frequencies given by the simulation were different from the previous models, which gave a greater understanding of the design problem and solution. Researchers have different approaches when including the SSI in their work. Previous works that include SSI show that there are many factors that needs to be taken into consideration. Often there are simplifications which results in inaccurate results. (Gonzalez 2016) showed that by considering the soil to be in different layers with different characteristics instead of treating the soil as a uniform layer, the damping changed. (Xie et al. 2020) created a full-body model of a offshore wind turbine with monopile foundation with inclusion of SSI. The SSI was then included in the model as a rotational spring-damper system which are represented in figure 39

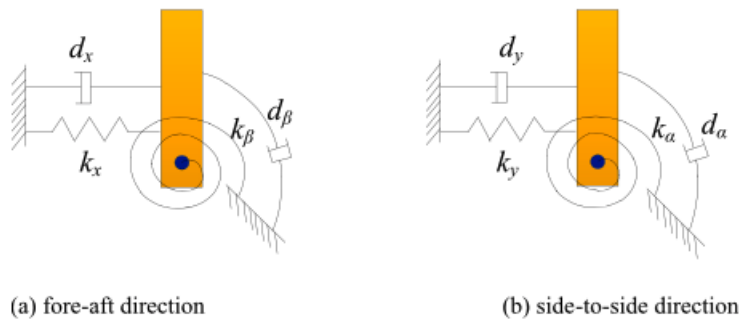


Figure 39: Simplified pile-soil interaction. (Xie et al. 2020)

3.10.6 0-Degrees of Freedom

The simplest way is to assume that the structure is fixed and therefore has 0 degrees of freedom. This method is a good starting point for any analysis but it has been shown that flexible soil can affect the dynamic response of the wind turbine. For example, the presence of flexible soil underneath the foundation of a structure increases the damping capacity of the foundation and reduces the structure's natural frequency (Veletsos AS. and Verbic 1973).

3.10.7 Multi-Degree of Freedom

Most commercial aerodynamic tools simplify the modelling of SSI by using six degrees of freedom at the base of the tower base for each vibrational mode combined with 6x6 stiffness and damping matrices. This approach is sufficient for a homogeneous elastic half space, but unsatisfactory for a layered soil. Some work related to inclusion of soil in modelling can be seen in (R. Nejad et al. 2018), (Damgaard et al. 2014), (Taddei et al. 2017), (Zuo et al. 2018). The articles include lumped mass models and modelling by conventional p-y, Q-z and t-z springs. (Wu and Lee 2002) gives a thorough introduction to lumped mass models, and may be studied further.

4 Standards

A standardization body is defined as an organization that in some way produces technical standards to address the needs of the industry. Some examples of international standards organizations are International Electrotechnical Commission (IEC) and the International Organization for Standardization (ISO). There are also non-governmental organizations that establish and maintain technical standards for offshore structures. There are also regional standardization organizations such as European Committee for Standardization (CEN) and national standardization organizations such as Norsk Elektroteknisk Komite (NEK) in Norway, Bundesamt für Seeschifffahrt und Hydrographie (BSH) in Germany and American Bureau of Shipping (ABS). ISO is a non-governmental international organization which provides more than 23 000 international standards (DNV-GL 2020). None of these standards are specific for wind turbines, but cover almost all aspects of manufacturing and technology. The IEC provides international standards for all electrical and electronic industries. A set of standards for wind turbines are included in the IEC 61400 - series. The BSH is responsible for testing and approval of power generating systems (offshore wind turbines), cables and other systems. The American Bureau for Shipping has three offshore specific documents:

- ABS Guide for Building and Classing Bottom-Founded Offshore Wind Turbine Installations.
- Guidance Notes on Global Performance Analysis for Floating Offshore Wind Turbine Installations.
- ABS Guide for Building and Classing Floating Offshore Wind Turbine Installations.

There are also Classification societies such as Bureau Veritas (BV), DNV and ClassNK (Nippon Kaiji Kyokai). BV and ClassNK has one specific document each for floating offshore wind: NI572 Classification and certification of floating offshore wind turbines and Guideline for Offshore Floating Wind Turbine Structures. DNV has the most extensive set of recommended practices and standards covering all assets in a wind power plant, including cables, turbines, offshore substations and bottom-fixed and floating support structures (DNV-GL 2020). An extensive list of relevant standards and guidance documents for bottom-fixed wind power plants can be seen in Appendix A.

4.1 Standards for Floating Wind Power Plants

The first standards for FOWTs were released between 2010-2013. In 2019 a technical specification was issued by the IEC. An overview of specific standards developed for FOWTs is seen in figure below.

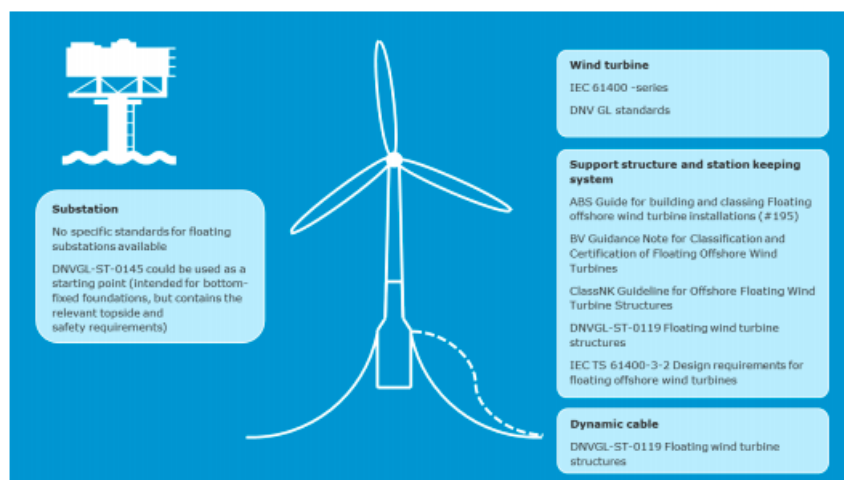


Figure 40: Overview of floating wind standards (DNV-GL 2020)

The standards contains contains various technical requirements. The BV standard includes recommendations for certification and classification and technical requirements. It was first issued October 2015, but was revised and re-issued in the beginning of 2019 including guidance on mechanical components. The guidance note covers floating platforms supporting any number of both vertical or horizontal axis turbines. However, it does not cover the blades, nacelle, rotor or tower design. The ClassNK guideline covers requirements for mooring, equipment, machinery installations, electrical installations, structural design and welding, loads, material, stability and external conditions including the tower. The technical specification IEC 61400-3-2 developed by the IEC was issued in 2019. It specifies design requirements for ensuring the engineering integrity of floating offshore wind turbines and requirements for assessment of the conditions at the FOWTs site. The purpose of the specification is to provide a level of protection against damage from all hazards during the FOWTs lifetime.

4.2 ABS

There are a number of environmental factors to be considered. Some of these include; wind, waves, currents, tides, air and sea temperatures, air density and seismic (American-Bureau-of-Shipping 2020). The wind conditions a wind turbine has to be designed for can be categorized into three conditions. Listed below (American-Bureau-of-Shipping 2020).

- The extreme wind conditions representing rare wind conditions with a given return point.
- The normal wind conditions, which occur more frequently than once per year.
- The survival wind conditions having a very low probability of being exceeded during the design life of the Floating Offshore Wind Turbine.

Further details are found in (American-Bureau-of-Shipping 2020).

For waves data needs to developed in order to determine the dynamic responses of the Floating Support Structure and stationkeeping system, fatigue, Wave impact of the structure and maximum responses of stationkeeping and structure system components. The design conditions are found in (American-Bureau-of-Shipping 2020) 4-3/3 through 4-3/9. Standards for loads are found in chapter 5. When considering wave loads TLP-type floating substructures the high-frequency wave loads has to be considered. This is because the waves may excite the structure at its natural periods in pitch, heave and roll. For other floating substructures the mean and oscillatory frequency drift forces may be determined using hydrodynamic computer programs (American-Bureau-of-Shipping 2020). Morrison ´s equation may be used for slender structures where the diameter is less than 20 percent of the wave lengths. A combination of diffraction and Morrison ´s equation can be used to calculate loading and characteristics from waves. To calculate the current force on a submerged structure the drag force is calculated by the following equation:

$$F_{current} = \frac{1}{2} \rho C_D A_{current} u_c |u_c| \quad (46)$$

where

- $F_{current}$ = current force in N
- ρ = mass density of water, kg/m^3
- C_D = drag coefficient in steady flow
- $A_{current}$ = projected area exposed to current in m^2
- u_c = current velocity vector normal to the plane of projected area, in m/s

4.3 DNV

The standard DNVGL-ST-0376 is the standard for rotor blades for wind turbines. It contains rules for design, materials, full scale blade testing, manufacturing, transport and installation, in-service inspections and maintenance, repair of manufacturing non-conformities and repair of in-service damages.

The DNVGL-ST-0119 has worldwide application. It is primarily concerned with the design of the main floater types and their moorings. It provides principles, technical requirements and guidance for design, construction and in-service inspection.

4.4 IEC 61400 series

The IEC 61400 is a series of standards which are to be followed. IEC 61400-1 is for wind energy generation systems. IEC 61400-3-1:2019 outlines the minimum design requirements for fixed offshore wind turbines. IEC TS 61400-3-2: Design requirements for floating wind turbines specifies essential design requirements to ensure the engineering integrity of floating offshore wind turbines and specifies additional requirements for analysing external conditions at a FOWT site. The document generally covers alternative floating platforms intended to support wind turbines and ship-shaped structures and barges, semi-submersibles, spar buoys and tension-leg platform. The document is applicable to unmanned floating structures with one single horizontal axis turbine. For vertical-axis wind turbines, combined wind/wave energy systems or multi-turbine units on a single floating substructure additional considerations are needed. The IEC 61400-5:2020 includes specifications to wind turbine blades. It include requirements for aerodynamic and structural design, material selection, evaluation and testing, manufacturing and transportation, installation, operation and maintenance of the blades.

5 Development Trend

There is a lot of research and development in the field of modelling and design of floating offshore wind turbines. This includes design methods, recommendations and software for multi-body simulation. The importance of modelling of coupled effects from wind, waves and current has produced several new software packages and extensions to current software.

There are currently more than 40 floating wind concepts under development. At the same time new concepts are frequently being announced. Some of these concepts challenge the leading concepts on factors as fabrication approach and mass while others are developing combined wind/wave systems or using multiple wind turbines on one floating support structure. There is also significant development in the mooring system. New materials and methods are proposed such as shared mooring, load reduction systems and synthetic ropes. These developments will enable floating wind levelised cost of energy(LCOE) to drop. It is estimated that the LCOE will be below 100 USD/MWh by 2025 and 40 USD/MWh by 2050 (DNV 2022a). Because the cost of materials is such a big part of the total cost of a wind turbine new designs using other materials are being developed. This will drive down costs and require new installation methods, standards and operating requirements. There are three main cost components that will contribute to lower costs. These are turbine costs, foundation cost and operational costs. Currently the operational cost is five times higher for floating wind compared to bottom fixed but an increase in turbine size and number of turbines will contribute to lower operational costs.

There is also constant development in the regulatory framework as new design concepts, materials, and tools are developed. We see that DNV is constantly revising their standards and pushing towards improved safety and operability. IEC 61400-3-2: Design requirements for floating wind turbines is also currently being worked on and the forecast publication date is 23-08-26. The document generally covers other floating platforms intended to support wind turbines. The document is applicable to unmanned floating structures with one single horizontal axis turbine. For vertical-axis wind turbines, combined wind/wave energy systems or multi-turbine units on a single floating substructure additional considerations are needed.

6 Discussion

With the transition towards renewable energy the offshore wind market will see huge growth. The different sectors within the industry will see many new developments and new standards are needed. As the program codes improve further designs can be developed. The MBS approach gives the opportunity to create a fully coupled multi body model. In SIMPACK the creation of such a model for a floating wind turbine including blades, tower, drivetrain, support structure, mooring lines, anchors and soil-structure interactions is challenging. These models are computationally demanding, and research suggest that simplifications can be implemented. Two of these implications are not including the drivetrain and simplifying the stationkeeping system. Applying this approach will greatly reduce the time and computational power needed for simulations and will in turn give the opportunity for faster iterations in the design stage. The model and simulation will also be less prone to errors. An example of software is the DNV software packages for OWTs. Here the floater substructure is modelled in Sesam and the hydrodynamic properties are determined. The coupled analysis of the complete system of wind turbine and floater is done in Bladed. The results from the coupled analysis can then be used in Sima for mooring and cable design, Sesam for analysis of the substructure and Bladed is used for the turbine design. The figure shows the design stages and software.

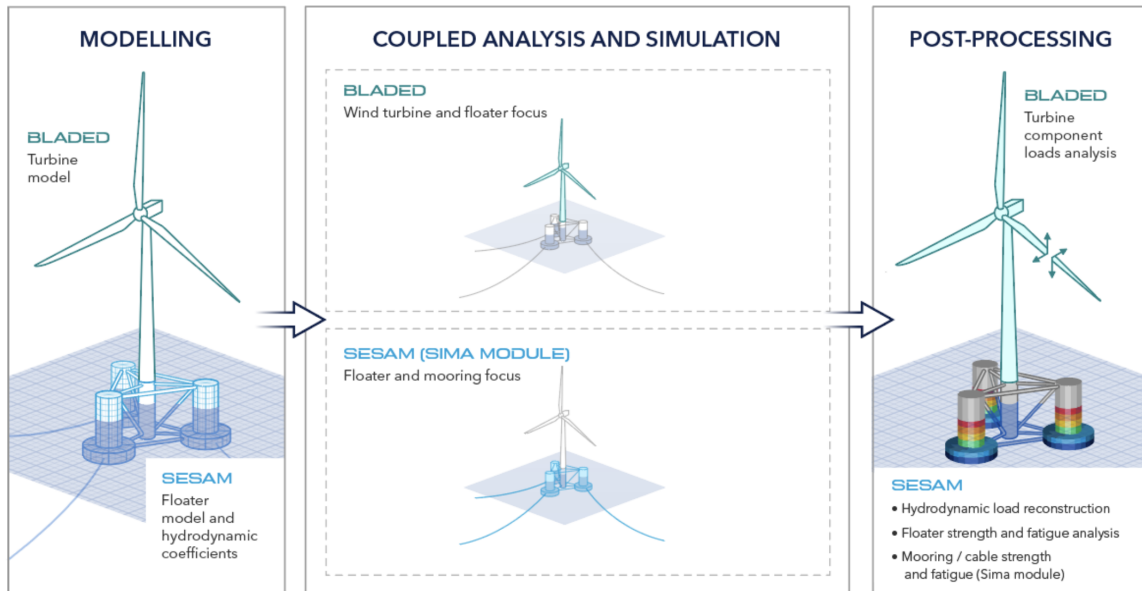


Figure 41: Workflow for floating offshore wind (DNV 2022b)

7 Conclusion

The wind energy is the fastest growing renewable energy sector. With the increasing focus on clean energy and current situation the world and Europe find themselves in, with growing inflation, higher gas and fuel prices, the shift towards sustainable energy been accelerated. There are increasing actors coming in to the field and focus on research to create better tools, regulatory framework, materials and make the production more efficient. Because of the high number of innovations and design solutions the computer aided design programs continues to see progress. We will see new solutions and improvement upon the existing ones. For modeling and simulation i propose to follow the DNV recommendations for modeling of offshore wind turbines. Because the offshore wind turbine farm design is so multidisciplinary an effort should be invested into understanding the theory and regulatory framework. For modeling and simulation of larger wind turbines one should use tools which enables fully coupled multi body simulation with aero-and hydrodynamic loads. The researched papers are divided on this issue. Some conclude that the drivetrain does not have to be taking into account, but as the rotation speed declines there might occur natural frequencies and modal modes where the design in insufficient. This may occur because of the influence of direct drive generators, anchor lines or motion of the floating support structure. For correct design and scaling formulas the regulatory framework by DNV and IEC61400 series should be followed. The current software models show that the impact of the drivetrain is small compared to other forces. The importance of detailed mooring system modeling is greater when using tension-leg floaters.

8 Further work

To gain deeper knowledge of the subject the next step i would suggest implementing the DNV software package and SIMPACK to model a floating offshore wind turbine. Several models could be created with changing simplifications. The models created in SIMPACK could be with simplified anchoring system, one model without the detailed modeling of the drivetrain and one model modeling all details. The DNV software package could also be implemented to have another reference point and the models could be compared. To further investigate the software and effect of simplifications several types of floating substructures could be modelled as the mooring system influences the different substructures differently. I believe that the comparison between tension-leg substructures and spar would show the biggest differences as the soil-structure interaction is of greater importance.

9 Appendix

9.1 Appendix A

Document code	Title
DNVGL-OS-C401	Fabrication and testing of offshore structures
DNVGL-RP-0043	Safety, operation and performance of grid-connected energy storage systems
DNVGL-RP-0286	Coupled analysis of floating wind turbines
DNVGL-RP-0360	Subsea power cables in shallow water
DNVGL-RP-0416	Corrosion protection for wind turbines
DNVGL-RP-0419	Analysis of grouted connections using the finite element method
DNVGL-RP-0423	Manufacturing and commissioning of offshore substations
DNVGL-RP-0440	Electromagnetic compatibility of wind turbines
DNVGL-RP-A203	Technology qualification
DNVGL-RP-D201	Integrated software dependent systems
DNVGL-ST-0054	Transport and installation of wind power plants
DNVGL-ST-0076	Design of electrical installations for wind turbines
DNVGL-ST-0119	Floating wind turbine structures
DNVGL-ST-0125	Grid code compliance

Figure 42: Wind turbine relevant standards and other guidance documents, bottom-fixed (DNV-GL 2020)

Document code	Title
DNVGL-ST-0126	Support structures for wind turbines
DNVGL-ST-0145	Offshore substations
DNVGL-ST-0262	Lifetime extension of wind turbines
DNVGL-ST-0358	Certification of offshore gangways for personnel transfer
DNVGL-ST-0359	Subsea power cables
DNVGL-ST-0437	Loads and site conditions wind for turbines
EN 50308	Wind Turbines – Protective Measures – Requirements for Design, Operation and Maintenance
IEC 60076 series	Power transformers
IEC 60227 series	Polyvinyl chloride insulated cables of rated voltages up to and including 450/750 V
IEC 60335-2-40	Household and similar electrical appliances - Safety - Part 2-40: Particular requirements for electrical heat pumps, air-conditioners and dehumidifiers
IEC 60364 series	Low-voltage electrical installations
IEC 60502 series	Power cables with extruded insulation and their accessories for rated voltages from 1 kV (Um= 1,2 kV) up to 30 kV (Um= 36 kV)
IEC 60751	Industrial platinum resistance thermometers and platinum temperature sensors
IEC 60870 series	Telecontrol equipment and systems
IEC 60947 series	Low-voltage switchgear and controlgear
IEC 60947-3	Low-voltage switchgear and controlgear - Part 3: Switches, disconnectors, switch-disconnectors and fuse-combination units
IEC 61131 series	Programmable controllers
IEC 61400-1	Wind energy generation systems- Part 1: Design requirements
IEC 61400-11	Wind turbines - Part 11: Acoustic noise measurements techniques
IEC 61400-12-1	Wind energy generation systems - Part 12-1: Power performance measurements of electricity producing wind turbines
IEC 61400-12-2	Wind turbines - Part 12-2: Power performance of electricity-producing wind turbines based on nacelle anemometry
IEC 61400-13	Wind turbines - Part 13: Measurement of mechanical loads
IEC 61400-14	Wind turbines - Part 14: Declaration of apparent sound power level and tonality values
IEC 61400-21	Wind turbines - Part 21: Measurement and assessment of power quality characteristics of grid connected wind turbines
IEC 61400-21-1	Wind turbines - Part 21: Measurement and assessment of power quality characteristics of grid connected wind turbines
IEC 61400-22	Wind turbines - Part 22: Conformity testing and certification of wind turbines
IEC 61400-23	Wind turbines - Part 23: Full-scale structural testing of rotor blades
IEC 61400-24	Wind turbines - Part 24: Lightning protection
IEC 61400-25 series	Wind energy generation systems - Communications for monitoring and control of wind power plants
IEC 61400-26-1	Wind energy generation systems – Part 26-1 IECRE Availability for wind energy generation systems
IEC 61400-27-1	Wind turbines - Part 27-1: Electrical simulation models - Wind turbines
IEC 61400-3-1	Wind energy generation systems - Part 3-1: Design requirements for fixed offshore wind turbines
IEC 61400-4	Wind turbines - Part 4: Design requirements for wind turbine gearboxes
IEC 61400-5	Wind energy generation systems - Part 5: Wind turbine blades
IEC 61400-6	Wind energy generation systems - Part 6: Tower and foundation design requirements

Figure 43: Wind turbine relevant standards and other guidance documents, bottom-fixed (continued) (DNV-GL 2020)

Document code	Title
IEC 61508 series	Functional safety of electrical/electronic/programmable electronic safety-related systems
IEC 61511 series	Functional safety - Safety instrumented systems for the process industry sector
IEC 62040 series	Uninterruptible power systems (UPS)
IEC 62053 series	Electricity metering equipment (a.c.) - Particular requirements
IEC 62271 series	High-voltage switchgear and control gear
IEC 62305 series	Protection against lightning
IEC 62477-1	Safety requirements for power electronic converter systems and equipment - Part 1: General
IEC 62610	Mechanical structures for electronic equipment - Thermal management for cabinets in accordance with IEC 60297 and IEC 60917 series
IEC/IEEE 82079-1	Preparation of information for use (Instructions for use) of products - Part 1: Principles and general requirements
IECRE CBC 6A	IEC Clarification sheet: Project certification recognition arrangement
ISO 3834-2	Quality requirements for fusion welding of metallic materials — Part 2: Comprehensive quality requirements
ISO 5149 series	Refrigerating systems and heat pumps - Safety and environmental requirements
ISO/IEC 13273-1	Energy efficiency and renewable energy sources - Common international terminology - Part 1: Energy efficiency
ISO/IEC 13273-2	Energy efficiency and renewable energy sources - Common international terminology - Part 2: Renewable energy sources

Figure 44: Wind turbine relevant standards and other guidance documents, bottom-fixed (continued) (DNV-GL 2020)

Document code	Title
API RP 2X	Recommended Practice for Ultrasonic and Magnetic Examination of Offshore Structural Fabrication and Guidelines for Qualification of Technicians
API RP 75	Safety and Environmental Management System for Offshore Operations and Assets
API Spec 2W	Specification for Steel Plates for Offshore Structures, Produced by Thermo-Mechanical Control Processing (TMCP)
API Spec 2Y	Specification for Steel Plates, Quenched-and-Tempered, for Offshore Structures
ASTM E1529	Standard Test Methods for Determining Effects of Large Hydrocarbon Pool Fires on Structural Members and Assemblies
CAP 437	Standards for offshore helicopter landing areas
CIGRE Technical Brochure 483	Guidelines for the Design and Construction of AC Offshore Substations for Wind Power Plants
CIGRE Technical Brochure 502	High-Voltage On-Site Testing with Partial Discharge Measurement
CIGRE Technical Brochure 537	Guide for Transformer Fire Safety Practices
DIN 50930-6	Corrosion of metals - Corrosion of metallic materials under corrosion load by water inside of pipes, tanks and apparatus - Part 6: Evaluation process and requirements regarding the hygienic suitability in contact with drinking water
DNVGL-OS-A101	Safety principles and arrangements
DNVGL-OS-A301	Human comfort
DNVGL-OS-B101	Metallic materials
DNVGL-OS-C101	Design of offshore steel structures, general - LRFD method
DNVGL-OS-C301	Stability and watertight integrity
DNVGL-OS-C401	Fabrication and testing of offshore structures
DNVGL-OS-D101	Marine and machinery systems and equipment
DNVGL-OS-D201	Electrical installations
DNVGL-OS-D202	Automation, safety and telecommunication systems
DNVGL-OS-D301	Fire protection

Figure 45: Offshore substation relevant standards and other guidance documents (DNV-GL 2020)

Document code	Title
DNVGL-OS-E401	Helicopter decks
DNVGL-RP-0360	Subsea power cables in shallow water
DNVGL-RP-0416	Corrosion protection for wind turbines
DNVGL-RP-0419	Analysis of grouted connections using the finite element method
DNVGL-RP-0423	Manufacturing and commissioning of offshore substations
DNVGL-RP-0423	Manufacturing and commissioning of offshore substations
DNVGL-RP-A203	Technology qualification
DNVGL-RP-B401	Cathodic protection design
DNVGL-RP-C204	Structural design against accidental loads
DNVGL-RP-C205	Environmental conditions and environmental loads
DNVGL-RP-C210	Probabilistic methods for planning of inspection for fatigue cracks in offshore structures
DNVGL-RP-C212	Offshore soil mechanics and geotechnical engineering
DNVGL-RU-SHIP Pt.4 Ch.6	Piping systems
DNVGL-RU-SHIP Pt.6 Ch.5	Equipment and design features
DNVGL-ST-0054	Transport and installation of wind power plants
DNVGL-ST-0126	Support structures for wind turbines
DNVGL-ST-0145	Offshore substations
DNVGL-ST-0359	Subsea power cables for wind power plants
DNVGL-ST-0377	Shipboard lifting appliances
DNVGL-ST-0378	Offshore and platform lifting appliances
DNVGL-ST-C502	Offshore concrete structures
DNVGL-ST-N001	Marine operations and marine warranty
DNVGL-ST-N002	Site specific assessment of mobile offshore units for marine warranty
DNV-RP-C201	Buckling strength of plated structures
EN 10025-series	Hot rolled products of structural steels
EN 10160	Ultrasonic testing of steel flat product of thickness equal or greater than 6 mm (reflection method)
EN 10204	Metallic products - Types of inspection documents
EN 10210-series	Hot finished structural hollow sections
EN 10219	Cold formed welded steel structural hollow sections
EN 10225-series	Weldable structural steels for fixed offshore structures
EN 1090-2	Execution of steel structures and aluminium structures - Part 2: Technical requirements for steel structures
EN 12097	Ventilation for Buildings - Ductwork - Requirements for ductwork components to facilitate maintenance of ductwork systems
EN 12599	Ventilation for buildings - Test procedures and measurement methods to hand over air conditioning and ventilation systems
EN 1363-2	Fire resistance tests - Part 2: Alternative and additional procedures
EN 14986	Design of fans working in potentially explosive atmospheres
EN 1993-1-series	Eurocode 3: Design of steel structures
EN 353-1	Personal fall protection equipment - Guided type fall arresters including an anchor line - Part 1: Guided type fall arresters including a rigid anchor line
EN 353-2	Personal protective equipment against falls from a height - Part 2: Guided type fall arresters including a flexible anchor line
EN 50272-2	Safety requirements for secondary batteries and battery installations - Part 2: Stationary batteries
EN 50499	Procedure for the assessment of the exposure of workers to electromagnetic fields

Figure 46: Offshore substation relevant standards and other guidance documents (continued) (DNV-GL 2020)

Document code	Title
EN 50522	Earthing of power installations exceeding 1 kV a.c
EN 54-series	Fire detection and fire alarm systems
FSS Code	International Code for Fire Safety Systems
FTP Code	International Code for Application of Fire Test Procedures
IACS UI SC241	Manually operated call points (SOLAS II-2/7.7)
IACS UR D11	Safety features
IACS UR D8	Hazardous areas
IACS UR E15	Electrical services required to be operable under fire conditions and fire resistant cables
IACS UR F29	Non-sparking fans
IACS UR P1	Rules for pipes
IEC 60076-series	Power transformers
IEC 60079-10-1	Explosive atmospheres - Part 10-1: Classification of areas - Explosive gas atmospheres
IEC 60079-14	Explosive atmospheres - Part 14: Electrical installations design, selection and erection
IEC 60092-series	Electrical installations in ships
IEC 60099-series	Surge arresters - Part 4
IEC 60331-series	Tests for electric cables under fire conditions. Circuit integrity
IEC 60332-3-series	Tests on electric and optical fibre cables under fire conditions
IEC 60364-7-701	Low-voltage electrical installations - Part 7: Requirements for special installations or locations
IEC 60364-series	Low-voltage electrical installations
IEC 60376	Specification of technical grade sulphur hexafluoride (SF6) and complementary gases to be used in its mixtures for use in electrical equipment
IEC 60502-2	Power cables with extruded insulation and their accessories for rated voltages from 1 kV (Um = 1,2 kV) up to 30 kV (Um = 36 kV) - Part 2: Cables for rated voltages from 6 kV (Um = 7,2 kV) up to 30 kV (Um = 36 kV)
IEC 60598-series	Luminaires
IEC 60700-1	Thyristor valves for high voltage direct current (HVDC) power transmission - Part 1: Electrical testing
IEC 60812	Failure modes and effects analysis (FMEA and FMECA)
IEC 60840	Power cables with extruded insulation and their accessories for rated voltages above 30 kV (Um = 36 kV) up to 150 kV (Um = 170 kV) - Test methods and requirements
IEC 60865-1	Short-circuit currents - Calculation of effects - Part 1: Definitions and calculation methods
IEC 60871-series	Shunt capacitors for a.c. power systems having a rated voltage above 1 000 V
IEC 61000-series	Electromagnetic compatibility (EMC)
IEC 61025	Fault tree analysis (FTA)
IEC 61071	Capacitors for power electronics
IEC 61400-3-1	Wind energy generation systems - Part 3-1: Design requirements for fixed offshore wind turbines
IEC 61643-11	Low-voltage surge protective devices - Part 11: Surge protective devices connected to low-voltage power systems - Requirements and test methods
IEC 61643-21	Low-voltage surge protective devices- Part 21: Surge protective devices connected to telecommunications and signaling networks - Performance requirements and testing methods
IEC 61869-series	Instrument transformers
IEC 61892-series	Mobile and fixed offshore units - Electrical installations
IEC 61936-1	Power installation exceeding 1 kVa.c. - Part 1: common rules
IEC 62067	Power cables with extruded insulation and their accessories for rated voltages above 150 kV (Um = 170 kV) up to 500 kV (Um = 550 kV) - Test methods and requirements
IEC 62271-series	High-voltage switchgear and control gear

Figure 47: Offshore substation relevant standards and other guidance documents (continued) (DNV-GL 2020)

Document code	Title
IEC 62305-1	Protection against lightning - Part 1: General principles
IEC 62305-3	Protection against lightning - Part 3: Physical damage to structures and life hazard
IEC 62305-4	Protection against lightning - Part 4: Electrical and electronic systems within structures
IEC 62485-series	Safety requirements for secondary batteries and battery installations
IEC 62501	Voltage sourced converter (VSC) valves for high-voltage direct current (HVDC) power transmission - Electrical testing
IEC TR 62001-series	High-voltage direct current (HVDC) systems - Guidance to the specification and design evaluation of AC filters
ISO 12944 series	Paints and varnishes - Corrosion protection of steel structures by protective paint systems
ISO 14122-series	Safety of machinery - Permanent means of access to machinery
ISO 14224	Petroleum, petrochemical and natural gas industries - Collection and exchange of reliability and maintenance data for equipment
ISO 14520-1	Gaseous fire-extinguishing systems — Physical properties and system design — Part 1: General requirements
ISO 15138	Petroleum and natural gas industries - Offshore production installations. Heating, ventilation and air-conditioning
ISO 1716	Reaction to fire tests for products — Determination of the gross heat of combustion (calorific value)
ISO 17631	Ships and marine technology - Shipboard plans for fire protection, life-saving appliances and means of escape
ISO 19900	Petroleum and natural gas industries - General requirements for offshore structures
ISO 19901-2	Petroleum and natural gas industries - Specific requirements for offshore structures
ISO 19902	Petroleum and natural gas industries - Fixed steel offshore structures
ISO 20902-1	Fire test procedures for divisional elements that are typically used in oil, gas and petrochemical industries — Part 1: General requirements
ISO 7547	Ships and marine technology — Air-conditioning and ventilation of accommodation spaces — Design conditions and basis of calculations
ISO 8861	Shipbuilding - Engine room ventilation in diesel-engined ships - Design requirements and basis of calculations
ISO 8862	Air-conditioning and ventilation of machinery control rooms on board ships - Design conditions and basis of calculations
ISO 9001	Quality management systems - Requirements
ISO 9943	Shipbuilding - Ventilation and air treatment of galleys and pantries with cooking appliances
ISO/IEC 17025	General requirements for the competence of testing and calibration laboratories
LSA Code	International Life-Saving Appliance (LSA) Code
MARPOL 73/78	International Convention for the Prevention of Pollution from Ships, 1973, as modified by the Protocol of 1978 as amended, including Annex V: Prevention of Pollution by Garbage from Ships
MODU Code	Code for the Construction and Equipment of Mobile Offshore Drilling Units
NFPA 11	Standard for Low-, Medium-, and High-Expansion Foam
NFPA 13	Standard for the Installation of Sprinkler Systems
NFPA 15	Standard for Water Spray Fixed Systems for Fire Protection
NFPA 16	Standard for the Installation of Foam-Water Sprinkler and Foam-Water Spray Systems

Figure 48: Offshore substation relevant standards and other guidance documents (continued) (DNV-GL 2020)

Document code	Title
NFPA 20	Standard for the Installation of Stationary Pumps for Fire Protection
NFPA 2001	Standard for Clean Agent Fire Extinguishing Systems
NFPA 750	Standard on Water Mist Fire Protection Systems
NORSOK C-001	Living quarter area
NORSOK C-002	Architectural components and equipment
NORSOK H-003	Heating, ventilation and air conditioning (HVAC) and sanitary systems
NORSOK M-501	Surface preparation and protective coating
NORSOK N-004	Design of steel structures
NORSOK S-002	Working environment
SOLAS	International Convention for the Safety of Life at Sea
VDI 6023	Hygiene in drinking-water installations - Requirements for planning, execution, operation and maintenance
Vds 2109	VdS Guidelines for Water Spray Systems - Planning and Installation
Vds 2380	VdS Guidelines for Fire Extinguishing Systems - Fire Extinguishing Systems Using Non-liquefied Inert Gases - Planning and Installation
VDS 2381	VdS Guidelines for fire extinguishing systems - Fire Extinguishing Systems using Halocarbon Gases - Planning and Installation

Figure 49: Offshore substation relevant standards and other guidance documents (continued) (DNV-GL 2020)

Document code	Title
API RP 2A	Recommended Practice for Planning, Designing and Constructing Fixed Offshore Platforms – Working Stress Design
API RP 2RD	Dynamic Risers for Floating Production Systems
CIGRÉ Electra 189	Recommendations for tests of power transmission DC cables for a rated voltage up to 800 kV
CIGRÉ Technical Brochure 177	Accessories for HV cables with extruded insulation
CIGRÉ Technical Brochure 279	Maintenance for HV cables and accessories
CIGRÉ Technical	Third-party damage to underground and submarine cables
CIGRÉ Technical Brochure 415	Test procedures for HV transition joints for rated voltages 30 kV (Um = 36 kV) up to 500 kV (Um = 550 kV)
CIGRÉ Technical Brochure 476	Cable accessory workmanship on extruded high voltage cables
CIGRÉ Technical Brochure 490	Recommendations for testing of long AC submarine cables with extruded insulation for system voltage above 30 (36) to 500 (550) kV
CIGRÉ Technical Brochure 496	Recommendations for testing DC extruded cable systems for power transmission at a rated voltage up to 500 kV
CIGRÉ Technical	Guideline to maintaining the integrity of XLPE cable accessories
CIGRÉ Technical Brochure 610	Offshore generation cable connections
DNVGL-RP-0360	Subsea power cables in shallow water
DNVGL-RP-F401	Electrical power cables in subsea applications
DNVGL-ST-0359	Subsea power cables for wind power plants
DNVGL-ST-N001	Marine operations and marine warranty
ICPC Recommendation	Standardization of electronic formatting of route position lists

Figure 50: Power cables relevant standards and other guidance documents (DNV-GL 2020)

Document code	Title
ICPC Recommendation 3	Criteria to be applied to proposed crossings between submarine telecommunications cables and pipelines/power cables
ICPC Recommendation 9	Minimum technical requirements for a desktop study (also known as cable route study)
IEC 60183	Guide to the selection of high-voltage cables
IEC 60228	Conductors of insulated cables
IEC 60287-1-1	Electric cables - Calculation of the current rating - Part 1-1: Current rating equations (100% load factor) and calculation of losses - General
IEC 60287-2-1	Electric cables - Calculation of the current rating - Part 2-1: Thermal resistance - Calculation of thermal resistance
IEC 60287-3-2	Electric cables - Calculation of the current rating - Part 3-2: Sections on operating conditions - Economic optimization of power cable size
IEC 60300-1	Dependability management - Part 1: Dependability management systems
IEC 60502	Power cables with extruded insulation and their accessories for rated voltages from 1 kV (Um = 1,2 kV) up to 30 kV (Um = 36 kV)
IEC 60793	Optical fibres
IEC 60794	Optical fibre cables
IEC 60840	Power cables with extruded insulation and their accessories for rated voltages above 30 kV (Um = 36 kV) up to 150 kV (Um = 170 kV) - Test methods and requirements
IEC 61400-3	Wind turbines - Part 3: Design requirements for offshore wind turbines
IEC 62067	Power cables with extruded insulation and their accessories for rated voltages above 150 kV (Um = 170 kV) up to 500 kV (Um = 550 kV) - Test methods and requirements
IMCA M 190	Guidance for Developing and Conducting Annual DP Trials Programmes for DP Vessels
IMO MSC/Circ.645	Guidelines for vessels with dynamic positioning systems
ISO 13628-5	Petroleum and natural gas industries - Design and operation of subsea production systems - Part 5: Subsea umbilicals
ISO 14688-1	Geotechnical investigation and testing - Identification and classification of soil - Part 1: Identification and description
ISO 14688-2	Geotechnical investigation and testing - Identification and classification of soil - Part 2: Principles for a classification
ISO 19901-6	Petroleum and natural gas industries - Specific requirements for offshore structures - Marine Operations
ISO 9001	Quality management systems - Requirements
ITU-T G.976	Test methods applicable to optical fibre submarine cable systems

Figure 51: Power cables relevant standards and other guidance documents (continued) (DNV-GL 2020)

Bibliography

- American-Bureau-of-Shipping (June 2020). *Guide for Building and Classing Floating Offshore Wind Turbines*. Tech. rep.
- Azcona, José et al. (2017). ‘Impact of mooring lines dynamics on the fatigue and ultimate loads of three offshore floating wind turbines computed with IEC 61400-3 guideline’. In: *Wind Energy* 20.5, pp. 797–813. DOI: <https://doi.org/10.1002/we.2064>.
- Azcane, J. et al. (2013). *D4.21: State-of-the-art and implementation of design tools for floating structures*. Tech. rep.
- Bachynski, Erin (2020). ‘Basic aerodynamics for wind turbines’. In: *TMR03 - IDAWT*. Trondheim: NTNU. Chap. 4.
- Bak, C., H. Aagaard Madsen and J. Johansen (2001). ‘Influence from blade-tower interaction on fatigue loads and dynamics (poster)’. English. In: *Wind energy for the new millennium. Proceedings*. Ed. by P. Helm and A. Zervos. 2001 European Wind Energy Conference and Exhibition (EWEC ’01), EWEC’01 ; Conference date: 02-07-2001 Through 07-07-2001. WIP - Renewable Energies, pp. 394–397. ISBN: 88-900442-9-2. URL: <http://www.ewea.org/index.php?id=146>.
- Banerjee, Arundhuti et al. (2019). ‘Dynamic analysis of an offshore wind turbine under random wind and wave excitation with soil-structure interaction and blade tower coupling’. In: *Soil Dynamics and Earthquake Engineering* 125. ISSN: 0267-7261. DOI: <https://doi.org/10.1016/j.soildyn.2019.05.038>.
- Barooni, M., N. Ale Ali and T. Ashuri (2018). ‘An open-source comprehensive numerical model for dynamic response and loads analysis of floating offshore wind turbines’. In: *Energy* 154, pp. 442–454. ISSN: 0360-5442. DOI: <https://doi.org/10.1016/j.energy.2018.04.163>.
- Beyer, Friedemann, M. Arnold and P. Cheng (2013). ‘Analysis of floating offshore wind turbine hydrodynamics using coupled CFD and multibody methods’. In:
- Blundell, Mike and Damian Harty (2015). ‘Chapter 3 - Multibody Systems Simulation Software’. In: *The Multibody Systems Approach to Vehicle Dynamics (Second Edition)*. Ed. by Mike Blundell and Damian Harty. Second Edition. Oxford: Butterworth-Heinemann, pp. 87–184. ISBN: 978-0-08-099425-3. DOI: <https://doi.org/10.1016/B978-0-08-099425-3.00003-0>. URL: <http://www.sciencedirect.com/science/article/pii/B9780080994253000030>.
- Borg, Michael and Henrik Bredmose (Jan. 2015). *LIFES50+ D4.4: Overview of the numerical models used in the consortium and their qualification*. Tech. rep.
- Cao, Guangwei et al. (2020). ‘Dynamic responses of offshore wind turbine considering soil non-linearity and wind-wave load combinations’. In: *Ocean Engineering* 217. ISSN: 0029-8018. DOI: <https://doi.org/10.1016/j.oceaneng.2020.108155>.
- Carswell, W. et al. (2015). ‘Foundation damping and the dynamics of offshore wind turbine monopiles’. In: *Renewable Energy* 80, pp. 724–736. ISSN: 0960-1481. DOI: <https://doi.org/10.1016/j.renene.2015.02.058>.
- Christl, Johannes et al. (2015). ‘FEA–MBS–Coupling–Approach for Vehicle Dynamics’. In:
- Cruz, Joao and Mairead Atcheson (Jan. 2016). *Floating Offshore Wind Energy: The Next Generation of Wind Energy*. ISBN: 978-3-319-29396-7. DOI: 10.1007/978-3-319-29398-1.
- Damgaard, M. et al. (2014). ‘Effects of soil–structure interaction on real time dynamic response of offshore wind turbines on monopiles’. In: *Engineering Structures* 75, pp. 388–401. ISSN: 0141-0296. DOI: <https://doi.org/10.1016/j.engstruct.2014.06.006>.
- Dassault Systemes (2020). *Simpack - Simulia*. URL: <https://www.3ds.com/products-services/simulia/products/simpack/>.
- DNV (Dec. 2020). *Overview of offshore wind standards and certification requirements in selected countries*. Tech. rep.
- (Mar. 2022a). *Floating Offshore Wind, The next five years*. Tech. rep.
- (2022b). *Industry workflows for floating offshore wind*. URL: <https://www.dnv.com/software/services/software-for-offshore-wind/floating-offshore-wind.html>.
- DNV-GL (May 2019). *Recommended practice: Coupled analysis of floating wind turbines, DNVGL-RP-0286*. Tech. rep.
- (Dec. 2020). *Overview of Offshore Wind Standards and Certification Requirements in selected Countries*. Tech. rep.

-
- DTU Wind Energy Report (2013). *Description of the DTU 10 MW Reference Wind Turbine*. Tech. rep.
- Fitzgerald, Breiffni and Biswajit Basu (2016). ‘Structural control of wind turbines with soil structure interaction included’. In: *Engineering Structures* 111, pp. 131–151. ISSN: 0141-0296. DOI: <https://doi.org/10.1016/j.engstruct.2015.12.019>.
- Ghassempour, Mina, Giuseppe Failla and Felice Arena (2019). ‘Vibration mitigation in offshore wind turbines via tuned mass damper’. In: *Engineering Structures* 183, pp. 610–636. ISSN: 0141-0296. DOI: <https://doi.org/10.1016/j.engstruct.2018.12.092>.
- Gonzalez, M. L. (2016). ‘Seismic analysis of monopile-based offshore wind turbines including aero-elasticity and soil-structure interaction’. In:
- Hau, Erich (2006). ‘Mechanical Drive Train and Nacelle’. In: *Wind Turbines: Fundamentals, Technologies, Application, Economics*. Berlin, Heidelberg: Springer Berlin Heidelberg, pp. 253–318. ISBN: 978-3-540-29284-5. DOI: 10.1007/3-540-29284-5_8. URL: https://doi.org/10.1007/3-540-29284-5_8.
- IEA Wind (2020). *ABOUT TASK 30*. URL: <https://community.ieawind.org/task30/home>.
- Igwemezie, Victor, Ali Mehmanparast and Athanasios Kolios (2019). ‘Current trend in offshore wind energy sector and material requirements for fatigue resistance improvement in large wind turbine support structures – A review’. In: *Renewable and Sustainable Energy Reviews* 101, pp. 181–196. ISSN: 1364-0321. DOI: <https://doi.org/10.1016/j.rser.2018.11.002>.
- Jahangiri, V. and C. Sun (2019). ‘Integrated bi-directional vibration control and energy harvesting of monopile offshore wind turbines’. In: *Ocean Engineering* 178, pp. 260–269. ISSN: 0029-8018. DOI: <https://doi.org/10.1016/j.oceaneng.2019.02.015>.
- Jiang, Zhiyu et al. (2020). ‘Design, modelling, and analysis of a large floating dock for spar floating wind turbine installation’. In: *Marine Structures* 72. ISSN: 0951-8339. DOI: <https://doi.org/10.1016/j.marstruc.2020.102781>.
- Jonkman, B. and Buhl Jr (Jan. 2007). ‘TurbSim User’s Guide’. In: DOI: 10.2172/15020326.
- Jonkman, J. M. et al. (2015). ‘AeroDyn v15 User’s Guide and Theory Manual - Draft’. In: *NREL*.
- Jonkman, Jason (Jan. 2013). ‘New Modularization Framework for the FAST Wind Turbine CAE Tool: Preprint’. In: DOI: 10.2514/6.2013-202.
- Jonkman, Jason et al. (2009). *Definition of a 5-MW reference wind turbine for offshore system development*. Tech. rep. National Renewable Energy Lab.(NREL), Golden, CO (United States).
- Krämer, Erwin (1993). ‘Rolling-element Bearings’. In: *Dynamics of Rotors and Foundations*. Berlin, Heidelberg: Springer Berlin Heidelberg, pp. 129–141. ISBN: 978-3-662-02798-1. DOI: 10.1007/978-3-662-02798-1_9. URL: https://doi.org/10.1007/978-3-662-02798-1_9.
- Kumar, Yogesh et al. (2016). ‘Wind energy: Trends and enabling technologies’. In: *Renewable and Sustainable Energy Reviews* 53, pp. 209–224. ISSN: 1364-0321. DOI: <https://doi.org/10.1016/j.rser.2015.07.200>. URL: <http://www.sciencedirect.com/science/article/pii/S1364032115009016>.
- Leishman, J. G. and T. S. Beddoes (1989). ‘A Semi-Empirical Model for Dynamic Stall’. In: *Journal of the American Helicopter Society*.
- Lemmer, Frank et al. (2020). ‘Multibody modeling for concept-level floating offshore wind turbine design’. In: *Multibody Syst Dyn* 49, pp. 203–236. DOI: <https://doi.org/10.1007/s11044-020-09729-x>.
- Ma, Kai-Tung et al. (2019). ‘Chapter 2 - Types of mooring systems’. In: ed. by Kai-Tung Ma et al., pp. 19–39. DOI: <https://doi.org/10.1016/B978-0-12-818551-3.00002-8>.
- Marsh, George (2005). ‘Wind turbines: How big can they get?’ In: *Refocus* 6.2, pp. 22–28. ISSN: 1471-0846. DOI: [https://doi.org/10.1016/S1471-0846\(05\)00326-4](https://doi.org/10.1016/S1471-0846(05)00326-4). URL: <http://www.sciencedirect.com/science/article/pii/S1471084605003264>.
- Matha, Denis et al. (Jan. 2011). ‘Challenges in Simulation of Aerodynamics, Hydrodynamics, and Mooring-Line Dynamics of Floating Offshore Wind Turbines’. In: *Proceedings of the International Offshore and Polar Engineering Conference*.
- Moan, T. et al. (2019). ‘Recent Advances in Response Analysis of Floating Wind Turbines in a Reliability Perspective’. In:
- Moriarty, P. J. and A. C. Hansen (2005). *AeroDyn Theory Manual*. Tech. rep.
- MSC Software (2020). *Adams*. URL: <https://www.mssoftware.com/product/adams>.
- Nejad, Amir Rasekhi (2018). ‘Modelling and analysis of drivetrains in offshore wind turbines’. In: *Offshore wind energy technology* 37.
- Nejad, Amir Rasekhi, Erin E. Bachynski et al. (2015). ‘Stochastic dynamic load effect and fatigue damage analysis of drivetrains in land-based and TLP, spar and semi-submersible floating
-

-
- wind turbines'. In: *Marine Structures* 42, pp. 137–153. ISSN: 0951-8339. DOI: <https://doi.org/10.1016/j.marstruc.2015.03.006>. URL: <http://www.sciencedirect.com/science/article/pii/S0951833915000325>.
- Nejad, Amir Rasekhi, Yi Guo et al. (2016). 'Development of a 5 MW reference gearbox for offshore wind turbines'. In: *Wind Energy* 19.6, pp. 1089–1106.
- Nejad, Amir Rasekhi, Torgeir Moan and CeSOS IMT (2012). 'Effect of geometrical imperfections of gears in large offshore wind turbine gear trains: 0.610 mw case studies'. In: *Proceedings of EWEA 2012*.
- Nejad, Amir Rasekhi, Yihan Xing et al. (2015). 'Effects of floating sun gear in a wind turbine's planetary gearbox with geometrical imperfections'. In: *Wind Energy* 18.12, pp. 2105–2120.
- NREL (2010). *Wind Power Today*. Tech. rep.
- (2020). *OpenFast Documentation*. URL: <https://openfast.readthedocs.io/en/master/index.html> (visited on 2020).
- 'Offshore Wind Turbine Hydrodynamics Modeling in SIMPACK' (2013). In:
- Peeters, Joris, Dirk Vandepitte and Paul Sas (Apr. 2006). 'Analysis of internal drive train dynamics in a wind turbine'. In: *Wind Energy* 9, pp. 141–161. DOI: 10.1002/we.173.
- Pisanò, Federico (Sept. 2019). 'Input of advanced geotechnical modelling to the design of offshore wind turbine foundations'. In: DOI: 10.32075/17ECSMGE-2019-1109.
- Popko, Wojciech et al. (June 2018). 'Verification of a Numerical Model of the Offshore Wind Turbine From the Alpha Ventus Wind Farm Within OC5 Phase III'. In: DOI: 10.1115/OMAE2018-77589.
- R. Nejad, Amir et al. (June 2018). 'A Systematic Design Approach of Gripper's Hydraulic System Utilized in Offshore Wind Turbine Monopile Installation'. In: DOI: 10.1115/OMAE2018-77228.
- Ragheb, A. and M. Ragheb (2010). 'Wind turbine gearbox technologies'. In: *2010 1st International Nuclear Renewable Energy Conference (INREC)*, pp. 1–8. DOI: 10.1109/INREC.2010.5462549.
- Ramachandran, GKV et al. (2013). *Investigation of response amplitude operators for floating offshore wind turbines*. Tech. rep. National Renewable Energy Lab.(NREL), Golden, CO (United States).
- Rulka, Wolfgang (1990). 'SIMPACK — A Computer Program for Simulation of Large-motion Multibody Systems'. In: *Multibody Systems Handbook*. Ed. by Werner Schiehlen. Berlin, Heidelberg: Springer Berlin Heidelberg, pp. 265–284. ISBN: 978-3-642-50995-7. DOI: 10.1007/978-3-642-50995-7_16. URL: https://doi.org/10.1007/978-3-642-50995-7_16.
- Shabana, Ahmed A. (2013). *Dynamics of Multibody Systems*. 4th ed. Cambridge University Press. DOI: 10.1017/CBO9781107337213.
- Simpack (2020a). *225: Gear Pair - Documentation*.
- (2020b). *43: Bushing Cmp - Documentation*.
- (2020c). *About AeroDyn V15 - Documentation*.
- (2020d). *Available Integrators - Documentation*.
- (2020e). *Flexible Bodies - Documentation*.
- Simpack - Simulia (2020). *ABAQUS UNIFIED FEA*. URL: <https://www.3ds.com/products-services/simulia/products/abaqus/> (visited on 2020).
- Stewart, Gordon and Matthew Lackner (July 2013). 'Offshore Wind Turbine Load Reduction Employing Optimal Passive Tuned Mass Damping Systems'. In: *IEEE Transactions on Control Systems Technology* 21.4. Last updated - 2017-06-01, pp. 1090–1104.
- Sun, C. and V. Jahangiri (May 2018). 'Bi-directional vibration control of offshore wind turbines using a 3D pendulum tuned mass damper'. In: *Mechanical Systems and Signal Processing* 105. Last updated - 2019-12-13, p. 338.
- Taddei, Francesca, Marco Schauer and Lisanne Meinerzhagen (2017). 'A practical soil-structure interaction model for a wind turbine subjected to seismic loads and emergency shutdown'. In: *Procedia Engineering* 199. X International Conference on Structural Dynamics, EURO DYN 2017, pp. 2433–2438. ISSN: 1877-7058. DOI: <https://doi.org/10.1016/j.proeng.2017.09.369>.
- Taherian Fard, Elaheh et al. (Sept. 2018). 'Wind Turbine Drivetrains: A Glimpse of Existing Technologies'. In: pp. 977–983. DOI: 10.1109/ECCE.2018.8557505.
- Uski, Sanna et al. (Jan. 2004). 'Adjoint wind turbine modeling with ADAMS, Simulink and PSCAD/EMTDC'. In: vol. 1.
- Veers, P.S. (2011). '5 - Fatigue loading of wind turbines'. In: *Wind Energy Systems*. Ed. by John D. Sørensen and Jens N. Sørensen. Woodhead Publishing Series in Energy. Woodhead Publishing,
-

-
- pp. 130–158. ISBN: 978-1-84569-580-4. DOI: <https://doi.org/10.1533/9780857090638.1.130>. URL: <http://www.sciencedirect.com/science/article/pii/B9781845695804500053>.
- Veletsos AS. and B. Verbic (1973). ‘Vibration of viscoelastic foundations’. In: *Earthquake Engineering and Structural Dynamics*.
- Wang, Shuaishuai, Amir R Nejad, Erin E Bachynski et al. (2020). ‘Effects of bedplate flexibility on drivetrain dynamics: Case study of a 10 MW spar type floating wind turbine’. In: *Renewable Energy* 161, pp. 808–824.
- Wang, Shuaishuai, Amir R Nejad and Torgeir Moan (2019). ‘On initial design and modelling of a 10 MW medium speed drivetrain for offshore wind turbines’. In: *Journal of Physics: Conference Series*. Vol. 1356. 1. IOP Publishing, p. 012024.
- Wang, Xuefei and Jiale Li (2020). ‘Parametric study of hybrid monopile foundation for offshore wind turbines in cohesionless soil’. In: *Ocean Engineering* 218. ISSN: 0029-8018. DOI: <https://doi.org/10.1016/j.oceaneng.2020.108172>.
- Willis, D.J. et al. (2018). ‘Wind energy research: State-of-the-art and future research directions’. In: *Renewable Energy*, pp. 133–154. DOI: <https://doi.org/10.1016/j.renene.2018.02.049>. URL: <https://www.sciencedirect.com/science/article/pii/S0960148118301939>.
- Wind Europe (2020). *Wind Energy In Europe: Outlook To 2020*. Tech. rep. URL: <https://windeurope.org/about-wind/reports/wind-energy-in-europe-outlook-to-2020/%7B%5C#%7Ddownload>.
- Withee, Jon E (2004). *Fully coupled dynamic analysis of a floating wind turbine system*. Tech. rep. Massachusetts Inst of Tech Cambridge.
- Wu, Wen-Hwa and Wen-How Lee (2002). ‘Systematic lumped-parameter models for foundations based on polynomial-fraction approximation’. In: *Earthquake Engineering & Structural Dynamics* 31.7, pp. 1383–1412. DOI: <https://doi.org/10.1002/eqe.168>.
- Xie, Shuangyi et al. (2020). ‘Applying multiple tuned mass dampers to control structural loads of bottom-fixed offshore wind turbines with inclusion of soil-structure interaction’. In: *Ocean Engineering* 205, p. 107289. ISSN: 0029-8018. DOI: <https://doi.org/10.1016/j.oceaneng.2020.107289>.
- Xing, Yihan (2013). ‘Modelling and analysis of the gearbox in a floating spar-type wind turbine’. In:
- Zhang, Shining and Takeshi Ishihara (Jan. 2016). ‘Effects of multidirectional sea states and flexible foundation on dynamic response of floating offshore wind turbine system’. In:
- Ziegler, Pascal and Peter Eberhard (2011). ‘Investigation of Gears Using an Elastic Multibody Model with Contact’. In: *Multibody Dynamics: Computational Methods and Applications*. Ed. by Krzysztof Arczewski et al. Dordrecht: Springer Netherlands, pp. 309–327. ISBN: 978-90-481-9971-6. DOI: 10.1007/978-90-481-9971-6.15. URL: <https://doi.org/10.1007/978-90-481-9971-6.15>.
- Zuo, Haoran, Kaiming Bi and Hong Hao (2018). ‘Dynamic analyses of operating offshore wind turbines including soil-structure interaction’. In: *Engineering Structures* 157, pp. 42–62. ISSN: 0141-0296. DOI: <https://doi.org/10.1016/j.engstruct.2017.12.001>.